Supplemental Materials

include

Supplemental Methods and References
Supplemental Figures and Legends
Supplemental Video Legends
Supplemental Tables

Supplemental Methods

Transfection and selection for stable clones of HEK293 Tet-on G0, G1, G2, and empty vector

cDNAs of *APOL1* G0, G1, and G2 were inserted into the *Nhe*I- and *Sal*I-digested pTRE2hyg vector (Clontech, Mountain View, CA).[1] To obtain Tet-inducible cell lines stably expressing *APOL1*, HEK 293 Tet-On 3G cell lines (Clontech, Mountain View, CA) were transfected in 100 mm dishes at 30% confluence with 5 μg pTRE2hyg plasmid containing *APOL1* G0, G1, G2, and empty vector using Lipofectamine transfection reagent (Invitrogen, Waltham, MA) based on manufacturer instructions. Cells were selected with DMEM (Invitrogen) containing 10% FBS supplemented with 400 μg/ml G418 (Cellgro, Manassas, VA) and 100 ug/ml hygromycin B (Invitrogen, Waltham, MA) 24 h post-transfection. Selection medium was replaced every 48h for 20 days. Individual clones were isolated, expanded, and maintained in DMEM media with 10% FBS, 100 μg/ml G418 and 50 ug/ml hygromycin B (referred to as complete DMEM growth media). Eight clones were characterized for each variant; one clone per variant was selected for all experiments. Individual clones with G0, G1 and G2 *APOL1* genotypes and empty pTRE2hyg vector were analyzed for inducible *APOL1* expression by RT-PCR, immunoblot analysis, and immunofluorescence.

Total RNA isolation, quality control, and real-time PCR

Total RNA was isolated from HEK293 Tet-on cells using RNAeasy Mini Kit (Qiagen, Germany). The quantity and quality of isolated RNA were determined by ultraviolet spectrophotometry and electrophoresis, respectively, on the Nanodrop 2000 (Thermo Fisher Scientific, Wilmington, DE) and Agilent 2100 Bioanalyzer (Agilent Technologies, Santa Clara, CA).

To determine *APOL1* mRNA levels in cells, 200ng of RNA was reverse transcribed with random hexamer primers using the TaqMan RT kit (Applied Biosystems, Foster City, CA). Primers were designed to capture all known *APOL1* splice variants. RT-PCR in the presence of SYBRGreen was performed with a Roche 480 Real-Time PCR system (Roche Diagnostics, Germany) using 18S ribosomal RNA for normalization. Primer sequences were described previously.[2] The ΔΔCT method[3] was used to

quantify the relative levels of *APOL1* mRNA. Fold-changes were normalized to mRNA levels on HEK293 Tet-on G0 cells without Dox induction. All experiments were performed in triplicate and results expressed as mean ± SD if not specified.

After Dox dose titration experiments to induce comparable levels of *APOL1* expression with each genotype, HEK293 Tet-on 3G cell lines stably expressing G0, G1, and G2 were incubated with 0.0313, 0.0625, and 0.1250 μg/ml Dox (BD Biosciences, San Jose, CA), respectively, for 8h or 16h. *APOL1* G0, G1, and G2 mRNA and protein expression was induced to similar levels in HEK293 Tet-on cell lines because inconsistent levels would complicate comparisons of downstream pathways. Dox-induced *APOL1* G0 expression levels in HEK293 Tet-on cells were introduced to a high enough level to distinguish that from non-induced cells while the cell viability remained the same for cells with and without induction. This allowed post-induction gene expression patterns for G1 and G2 vs. G0 to be more readily detectable. The cell line stably transfected with empty pTRE2hyg plasmid was incubated with 0.25 μg/ml Dox to ensure absence of *APOL1* expression and serve as a control for gene expression studies. Inclusion of HEK293 empty pTRE2hyg vector Tet-on cells excluded significant transcript level changes related to Dox induction (data not shown), and ensured that altered gene expression in HEK293 Tet-on cells with and without Dox induction were attributed to over-expression of *APOL1* variants.

Cell viability assay

Stabilized HEK293 Tet-on *APOL1* G0, G1, G2 and empty vector cells (20,000/well) were seeded on three 96-well plates. After 24h of growth, cells were induced with Dox for 2hr, 4hr, 8hr or 16hr in complete DMEM media; non-induced cells were incubated with corresponding DMEM media without Dox. Cell viability was measured using Cytotox 96 LDH viability assay kit (Promega, Madison, WI) per manufacturer instructions. Each cell line (with and without Dox induction) was measured at least 6 times, with values expressed as mean ± SD on the bar graph. Full cell viability was defined as 1.0 (100% viable).

Global gene expression and pathway analyses

Total RNAs were isolated from HEK293 Tet-on cell lines stably expressing *APOL1* G0, G1, and G2 (and empty vector) cell lines with and without Dox induction. All 24 RNA samples (eight groups in triplicate, see **Supplemental Figure 1**) were processed on Illumina human HT-12 v4 arrays in a single batch according to manufacturer instructions. Six RNA samples (G0, G1 and G2, in duplicate) were examined on exon-based Affymetrix HTA2.0 arrays to confirm the findings from Illumina bead arrays. In addition, 53 samples of non-diseased primary proximal tubule cells (PTCs) from African Americans were processed on Affymetrix HTA2.0 arrays to determine whether the most differentially expressed genes attributed to *APOL1* renal-risk variants replicated findings in the HE293 Tet-on cell model. Since Illumina and Affymetrix arrays were done in the same batch, no batch effects were seen. The quality control analysis and normalization confirmed the absence of failed samples or outliers. Whole genome transcript intensity profiles were extracted using GenomeStudio V2011.1 for Illumina human HT-12 v4 arrays and Transcriptome Analysis Console (TAC) software for Affymetrix HTA 2.0 arrays, respectively. Levels of expression were estimated by RMA[4] normalized $\log_2$ converted probe set pixel intensity. The threshold for detectable transcripts was set at signal/noise ratio (SNR) greater than 3. The gene expression data of Illumina HT-12 v4 and Affymetrix HTA 2.0 arrays are available in the NCBI Gene Expression Omnibus (GEO) database.

Paired analysis between HEK293 Tet-on *APOL1* cell samples for differentially expressed genes were performed by empirical Bayers method[5] implemented in R Biocondoctor limma package, where the selection thresholds used were |logFC| >1 and FDR (False Discovery rate) p <0.01.

EPIG[6], a java-based gene expression profile clustering method was employed. It uses an un-supervised profile approach to extract patterns from whole data sets and then categorize the genes to one of the patterns if they met all of the following criteria: SNR > 3, corresponding p<0.005, absolute $\log_2$ fold change >1, and maximum Pearson correlation r value to a given pattern >0.87. This approach was applied to both Illumina and Affymetrix array data for RNA samples of Dox-induced G0, G1 and G2 cells. The former arrays were performed in triplicate and the later in duplicate; 14 and 11 patterns were extracted, respectively. Each pattern consisted of a set of genes which were highly similar in their

expression profiles, which may be co-expressed and relevant to biological co-regulation. Overall, fewer than 8% of expressed genes were selected from either array to form specific patterns, representing the high stringency of criterion settings for EPIG.

Both Cytoscape (http://www.cytoscape.org/) and Ingenuity pathway analysis (IPA) (http://www.ingenuity.com/) were performed to identify significant pathways relevant to G1 and G2.

Paired analysis between PTCs with 2 renal-risk alleles and those without risk alleles for differentially expressed genes were performed using the Affymetrix TAC package, where the selection thresholds employed were $|logFC| > 1.5$ and ANOVA $p < 0.005$.

Immunoblotting

Immunoblotting was performed as reported.[2] Briefly, blots were incubated overnight at 4°C with primary antibodies. The membranes were then washed three times in Tris-buffered saline containing 0.1% Tween 20 and incubated for 1h in blocking buffer with an anti-rabbit or mouse IgG secondary antibody conjugated to horseradish peroxidase (1:20,000; Jackson ImmunoResearch Laboratories, West Grove, PA). Detailed information on experimental conditions for primary antibodies used in immunoblot is provided in **Supplemental Table 12**. COX IV and VDAC1 served as mitochondrial content markers.[8,9]

Immunofluorescence

Immunofluorescence of APOL1 (Epitomics, Burlingame, CA) and mitochondrial marker ATP5A1 (Invitrogen, Frederick, MD) and other markers was performed on HEK293 Tet-on cell lines using established protocols.[2] Secondary antibodies (goat anti-rabbit Alexa Fluor 594 and goat anti-rabbit Alexa Fluor 488, Invitrogen) were used to display fluorescent signals (1:500 dilution). Microscopy was performed using a Zeiss LMS 710 confocal microscope (Oberkochen, Germany).

Fifty nM of mitotracker Green (Invitrogen) and 10 nM of TMRE (Invitrogen) were incubated with HEK293 Tet-on cells for 30 min prior to signal detection. Microscopy was performed using an

Olympus IX71 fluorescence microscope (Olympus Scientific Solutions Americas Corp., Waltham, Massachusetts).

Measurement of intracellular potassium concentrations

HEK293 Tet-on *APOL1* (G0, G1 and G2) cells were seeded on a 96 well plate pre-coated with Cell-Tak (Corning, Bedford, MA) at a density of 20,000 cells/well 24 hr prior to Dox induction. After 8 hr or 16 hr of Dox induction, Dox-induced and non-induced cells were incubated with a fluorescent potassium indicator (Asante Potassium Green-2 AM, APG-2 AM, Abcam, Cambridge, MA) for 30 min in 3% BSA-PBS (final concentration 2 μM) according to the manufacturer's instructions, followed by a 5 min gentle wash with PBS. The indicator was excited at 488 nm and fluorescent emission intensity was measured at 530 nm. Fluorescence signals were read on a BioTek Synergy-HTX multi-mode plate reader (BioTek, Winooski, VT). A standard curve was constructed based on measurements of fluorescent intensity in HEK293 G0 cells incubated with a 50 μM of amphotericin B, an ionophore, for 15 min for each $[K^+]$ standard concentration. Ionophore treatment allowed $[K^+]$ equilibration with known standard extracellular 50, 100 and 150 mM $[K^+]$ in 3% BSA-PBS. The standards were made in cell culture buffer in which NaCl ions were iso-osmotically replaced by KCl, keeping the osmolarity 300 mOsm/L. A standard curve was obtained from a series of triplicate wells of known ionophore-balanced intracellular $[K^+]$ on the same plate as G0, G1 and G2 cell samples, by plotting $[K^+]$ vs. fluorescent intensity and determining the line of best fit using linear regression (r^2=0.99). The fluorescent signals were normalized to cell lysate total protein in corresponding wells before being used for quantification of intracellular $[K^+]$. The measurement in each cell type (G0, G1 and G2; without and with Dox induction) was repeated in four wells, and the average of the four measurements is shown on the bar graph. P-values were assessed using ANOVA.

Supplemental References:

1. Cheng D, Weckerle A, Yu Y, Ma L, Zhu X, Murea M, Freedman BI, Parks JS, Shelness GS: Biogenesis and cytotoxicity of APOL1 renal risk variant proteins in hepatocytes and hepatoma cells. *J. Lipid Res.* 56: 1583–1593, 2015

2. Ma L, Shelness GS, Snipes JA, Murea M, Antinozzi PA, Cheng D, Saleem MA, Satchell SC, Banas B, Mathieson PW, Kretzler M, Hemal AK, Rudel LL, Petrovic S, Weckerle A, Pollak MR, Ross MD, Parks JS, Freedman BI: Localization of APOL1 protein and mRNA in the human kidney: nondiseased tissue, primary cells, and immortalized cell lines. *J. Am. Soc. Nephrol.* 26: 339–348, 2015

3. Livak KJ, Schmittgen TD: Analysis of relative gene expression data using real-time quantitative PCR and the 2(-Delta Delta C(T)) Method. *Methods* 25: 402–408, 2001

4. Bolstad BM, Irizarry RA, Astrand M, Speed TP: A comparison of normalization methods for high density oligonucleotide array data based on variance and bias. *Bioinforma.* 19: 185–193, 2003

5. Smyth GK: Linear models and empirical bayes methods for assessing differential expression in microarray experiments. *Stat. Appl. Genet. Mol. Biol.* 3: 3, 2004

6. Chou JW, Zhou T, Kaufmann WK, Paules RS, Bushel PR: Extracting gene expression patterns and identifying co-expressed genes from microarray data reveals biologically responsive processes. *BMC Bioinforma.* 8: 427, 2007

7. Maere S, Heymans K, Kuiper M: BiNGO: a Cytoscape plugin to assess overrepresentation of gene ontology categories in biological networks. *Bioinforma.* 21: 3448–3449, 2005

8. De Pablo-Latorre R, Saide A, Polishhuck EV, Nusco E, Fraldi A, Ballabio A: Impaired parkin-mediated mitochondrial targeting to autophagosomes differentially contributes to tissue pathology in lysosomal storage diseases. *Hum. Mol. Genet.* 21: 1770–1781, 2012

9. Converso DP, Taillé C, Carreras MC, Jaitovich A, Poderoso JJ, Boczkowski J: HO-1 is located in liver mitochondria and modulates mitochondrial heme content and metabolism. *FASEB J.* 20: 1236–1238, 2006

Supplemental Figures

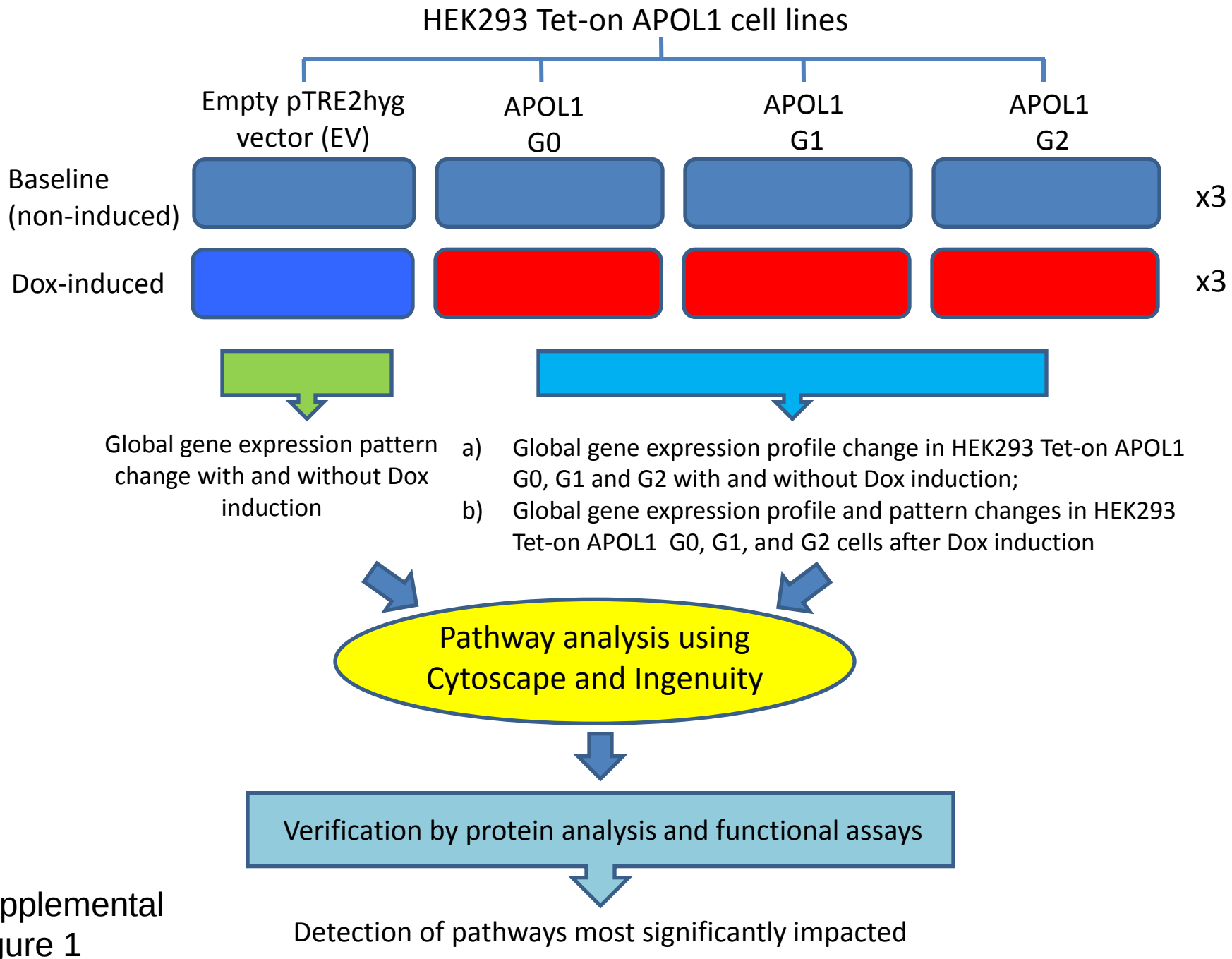

Supplemental Figure 1

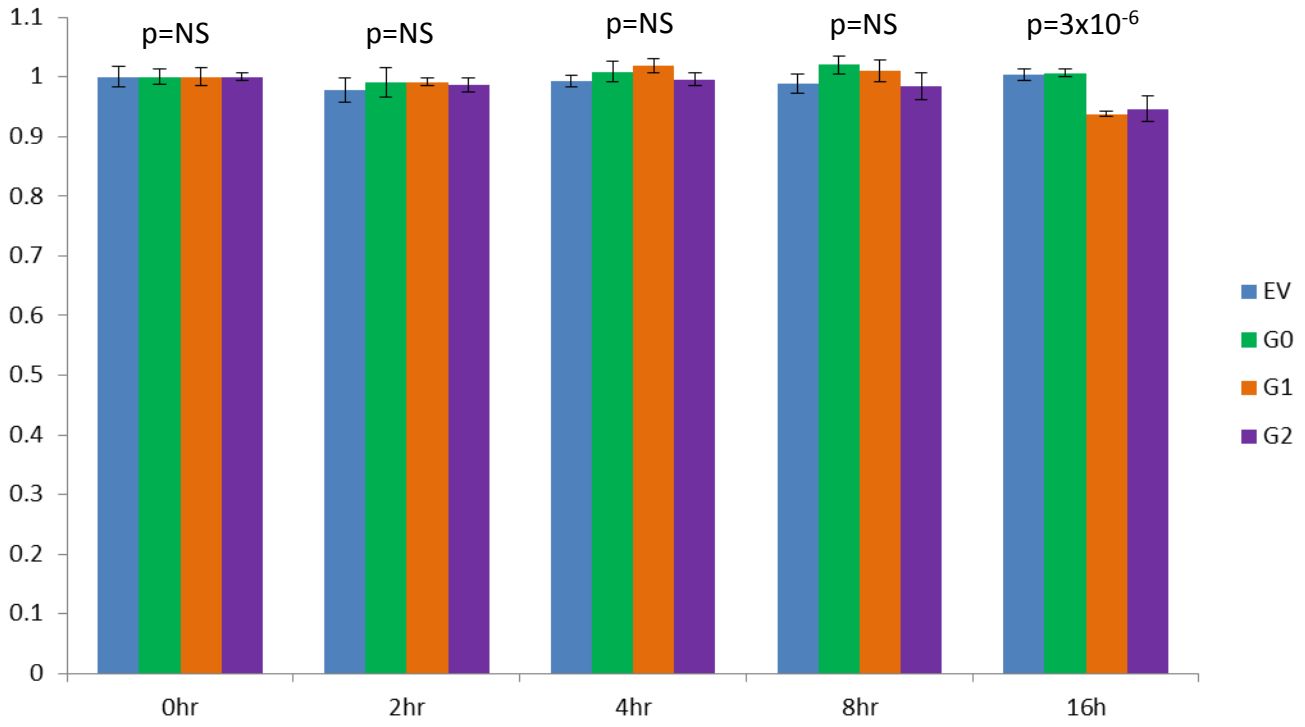

Supplemental Figure 2

Supplemental Figure 2. Quantitation of serial cell viability of HEK293 Tet-on G0, G1, or G2 cells with Dox induction at time point 0, 2, 4, 8 and 16 hr.

Stabilized HEK293 Tet-on *APOL1* G0, G1, G2 and empty vector (EV) cells were seeded on three 96-well plates at a density of 20,000/well. After 24h of growth, cells were induced with Dox for 2hr, 4hr, 8hr and 16hr, respectively, in complete DMEM media. Non-induced cells were incubated with corresponding DMEM media without Dox. Cell viability was measured using the Cytotox 96 LDH viability assay kit (Promega, Madison, WI) per manufacturer instructions. Each cell line (with and without Dox induction) was measured at least 6 times, with values expressed as mean ± SD on the bar graph. Full cell viability was defined as 1 (100%). NS: not significant ($p>0.05$).

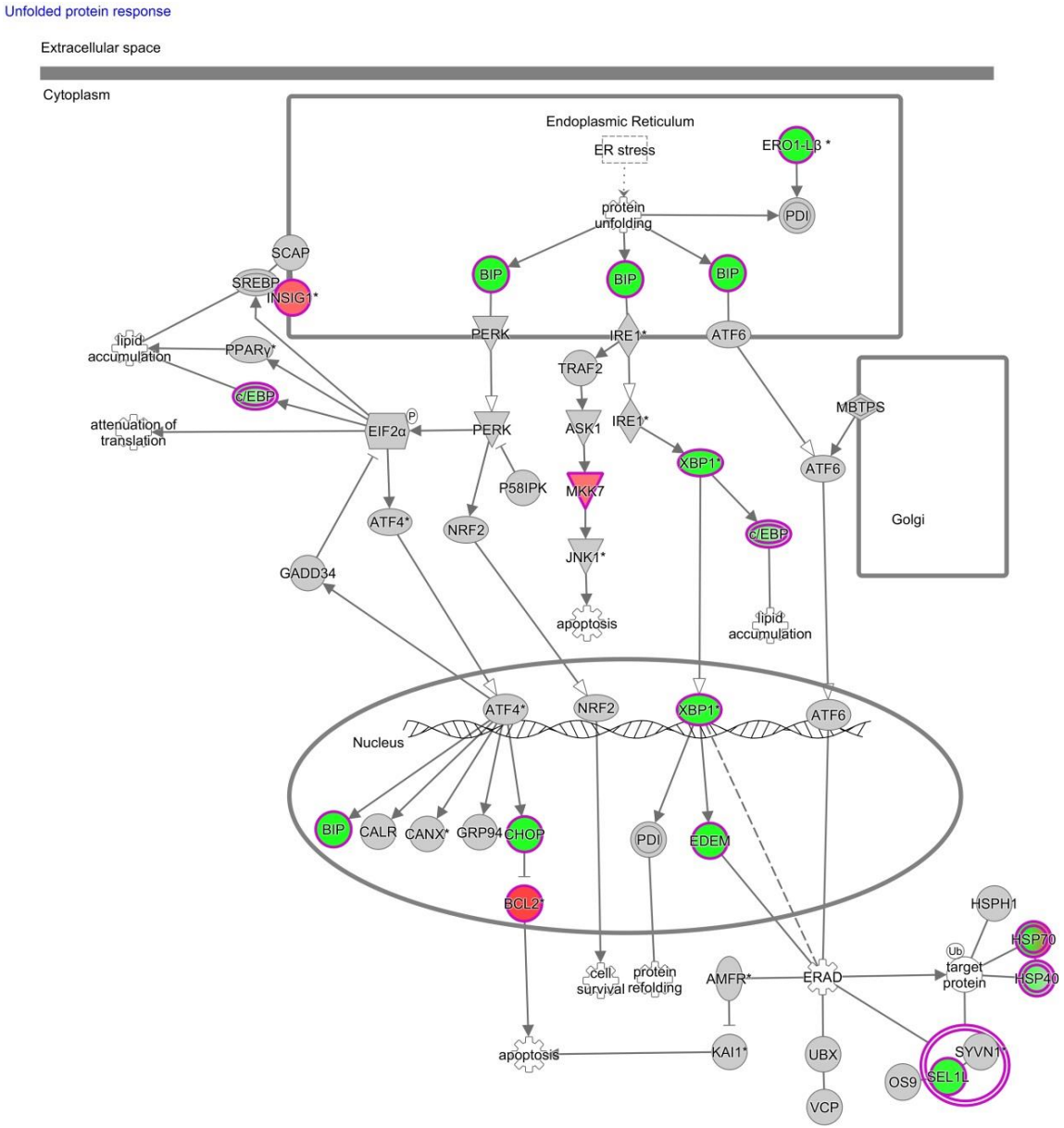

Supplemental Figure 3

Supplemental Figure 3. *APOL1* G0 inhibits the unfolded protein response (endoplasmic reticulum stress)
Down-regulation of the endoplasmic reticulum (ER) stress pathway by Dox-induced *APOL1* G0 over-expression is characterized by decreased ER stress sensor BiP, effector CHOP and chaperone HSP70/co-chaperone HSP40.

Pathway symbols are defined in Figure 3 legend.

A

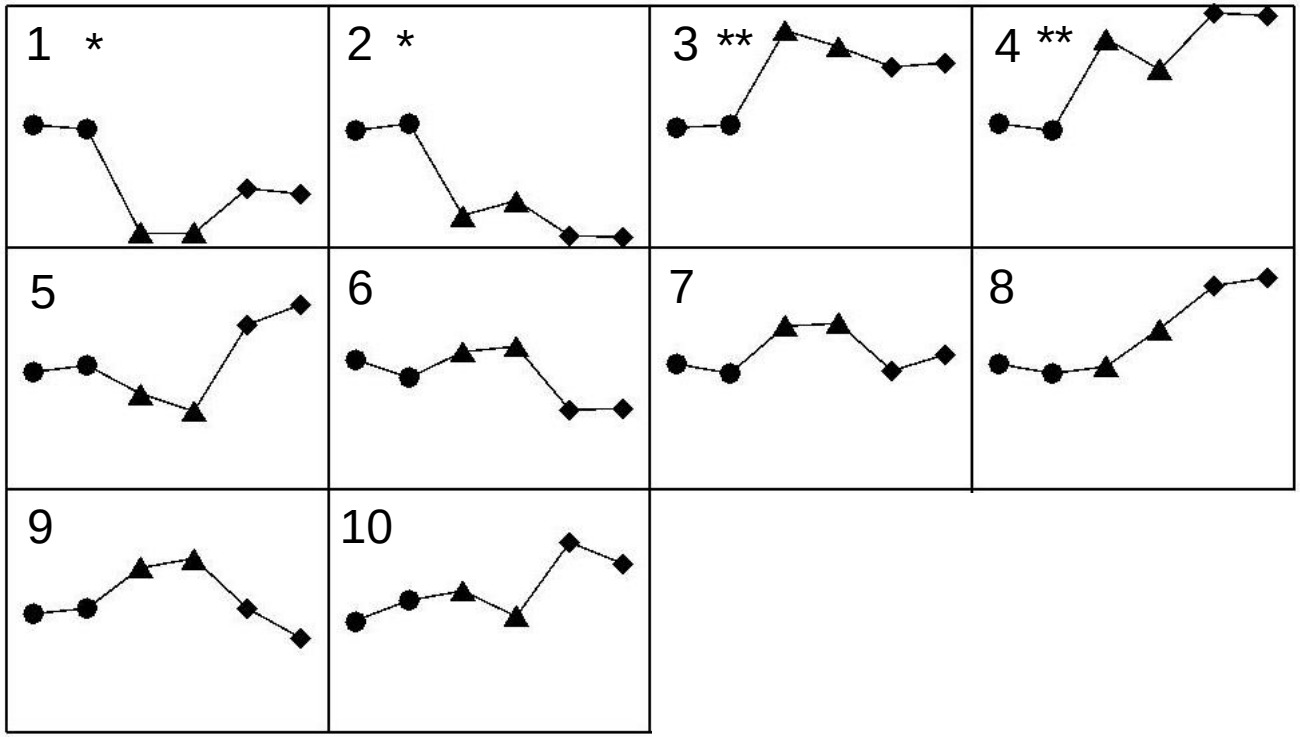

B

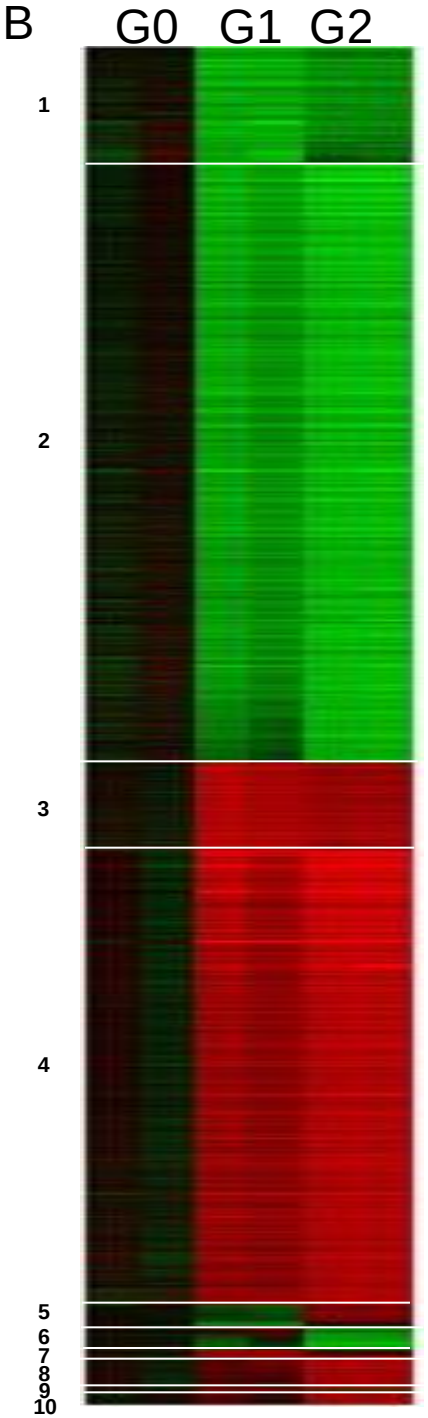

Supplemental
Figure 4

Supplemental Figure 4. Significantly clustered expression patterns for HEK293 Tet-on *APOL1* G0, G1, and G2 cells in pattern analysis on Affymetrix HT 2.0 arrays

A) Gene expression patterns most altered in HEK293 Tet-on *APOL1* G0 (circle), G1 (triangle), and G2 (diamond) cells with Dox induction. *Mitochondrial dysfunction is enriched in patterns 1 and 2; **Activated TGF-β signaling is enriched in patterns 3 and 4.

B) Heat map of clustered gene expression patterns from top to bottom includes 3620 transcripts, order from pattern 1 to 10. Transcript expression in G0 cells shown in black; red and green correspond to up or down regulated transcripts, respectively, in G1 or G2 cells. Lighter colors denote less differential expression.

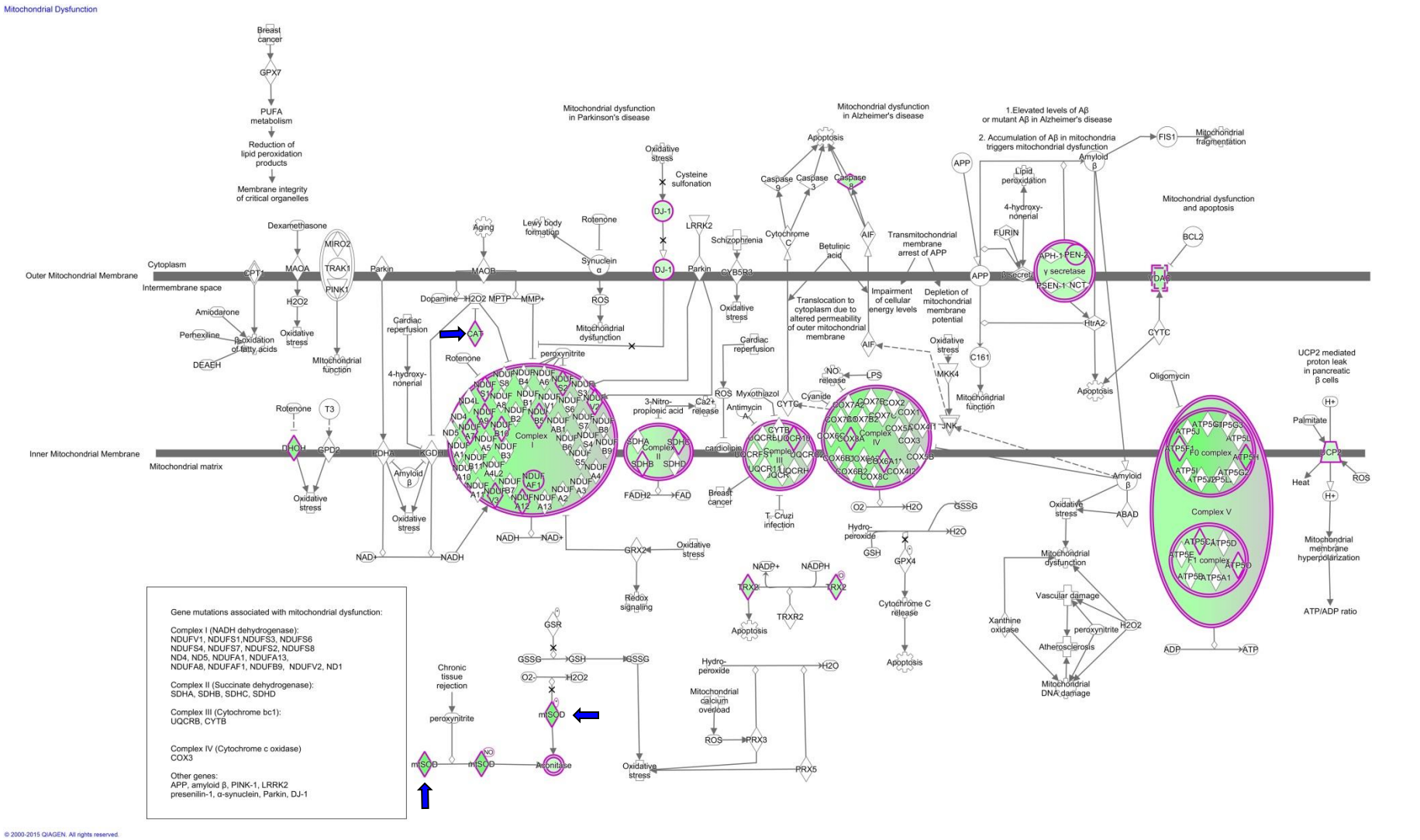

Supplemental
Figure 5

Supplemental Figure 5. *APOL1* G1 and G2 renal-risk variants contribute to mitochondrial dysfunction

Affymetrix array patterns 1 and 2 (Supplemental Figure 4) were analyzed using IPA for HEK293 Tet-on *APOL1* G1 and G2 vs. G0 cells. Results indicate marked down-regulation of enzymes in mitochondrial complexes I to V. In addition, mtSOD/*SOD2* and *CAT* (blue arrows) were down-regulated by *APOL1* renal-risk variants, suggesting a role for oxidative stress in *APOL1*-associated nephropathy.

Pathway symbols are defined in Figure 3 legend.

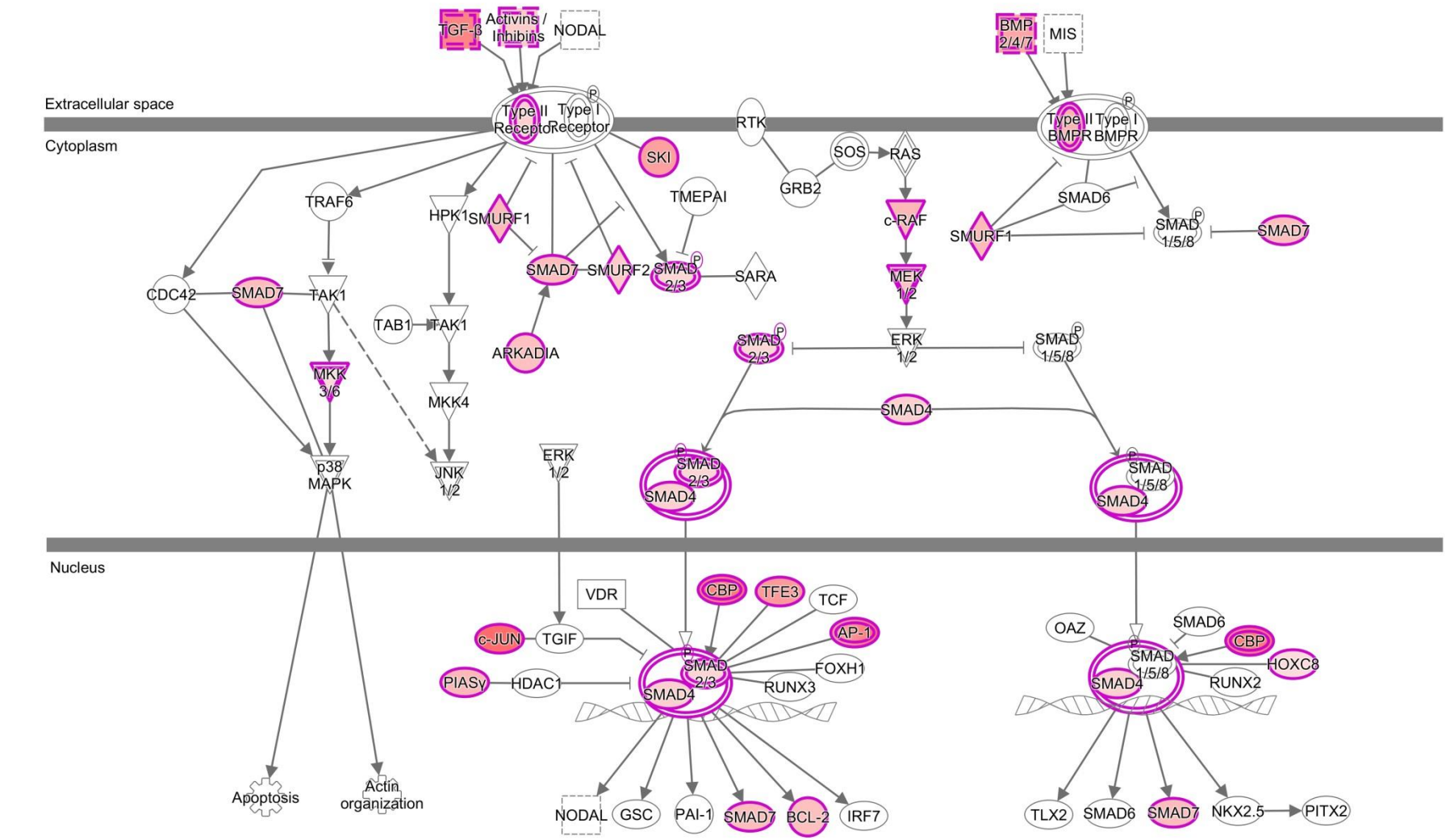

Supplemental Figure 6

Supplemental Figure 6. *APOL1* G1 and G2 renal-risk variants contribute to activated TGF-β signaling.

AFFY patterns 3 and 4 were analyzed using IPA for HEK293 Tet-on *APOL1* G1 and G2 vs. G0 cells. Results indicate up-regulation of transcripts in the canonical TGF-β signaling pathway.

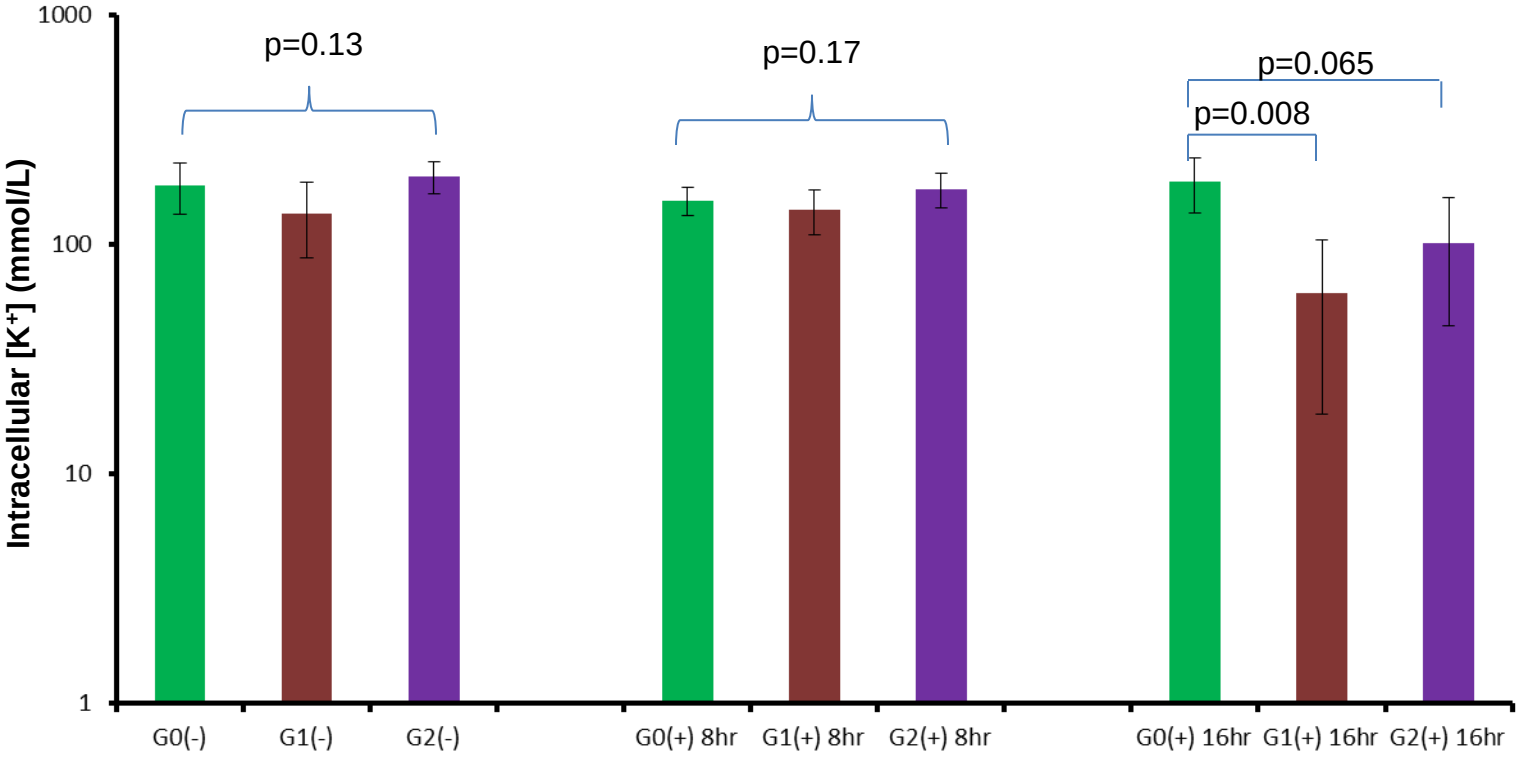

Supplemental
Figure 7

Supplemental Figure 7. Intracellular potassium concentrations for HEK293 Tet-on G0, G1, or G2 cells without Dox and with Dox induction for 8 and 16 hr.

Intracellular [K^+] was measured in quadruplicate with fluorescent potassium indicator (Asante Potassium Green-2 AM) for HEK293 Tet-on G0, G1 and G2 cells without and with Dox induction (8 hr and 16 hr). The intracellular potassium concentration [K^+] (in mmol/L) is $\log_{10}$ transformed on the y-axis.

No significant difference in [K^+] was observed among 16hr-Dox-induced G0 cells and non-induced or 8-hr-Dox-induced G0, G1 and G2 cells (ANOVA p=0.10), the estimated average intracellular [K^+] of which was 168.0±40.1 mmol/L (total n=28 in 7 groups). The estimated intracellular [K^+] for G1 and G2 cells with 16 hr Dox induction was reduced to 61.2±43.2 mmol/L (n=4) and 101.8±49.8 moml/L (n=4), respectively.

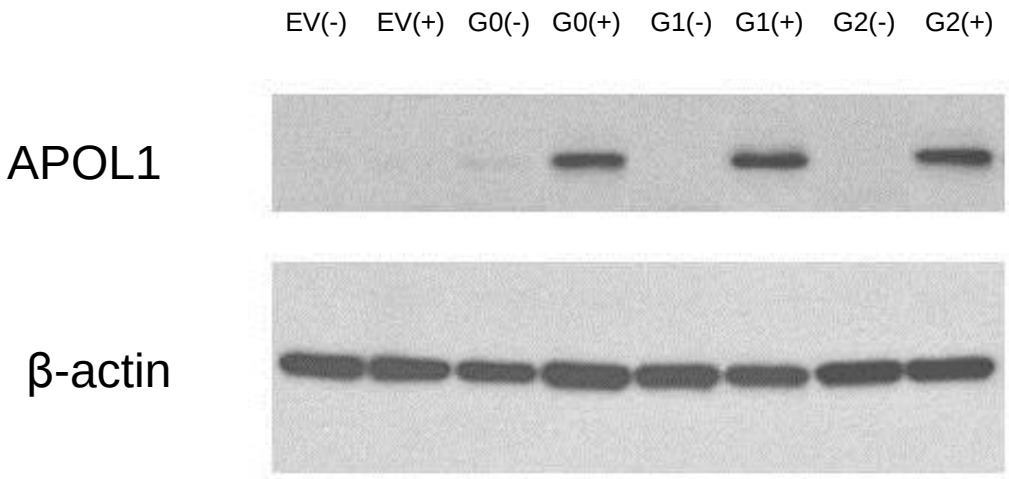

Supplemental Figure 8. Relative APOL1 expression level is comparable in HEK293 Tet-on cells with Dox induction for 8 hr. HEK293 Tet-on cells with (+) or without (-) Dox induction were grown in complete DMEM growth media for 8 hr. Four ug of total cell lysate protein was loaded onto a 4-20% SDS-PAGE gel and probed with APOL1 antibody. HEK293 Tet-on empty pTRE2hyg vector cells did not express APOL1 with or without Dox induction. HEK293 Tet-on APOL1 G0, G1, and G2 cells expressed similar amounts of APOL1 (elevated) with Dox induction, while trace or negligible amounts of APOL1 were present in HEK293 Tet-on cells without Dox induction. The data are representative of three trials of immunoblot with similar results.

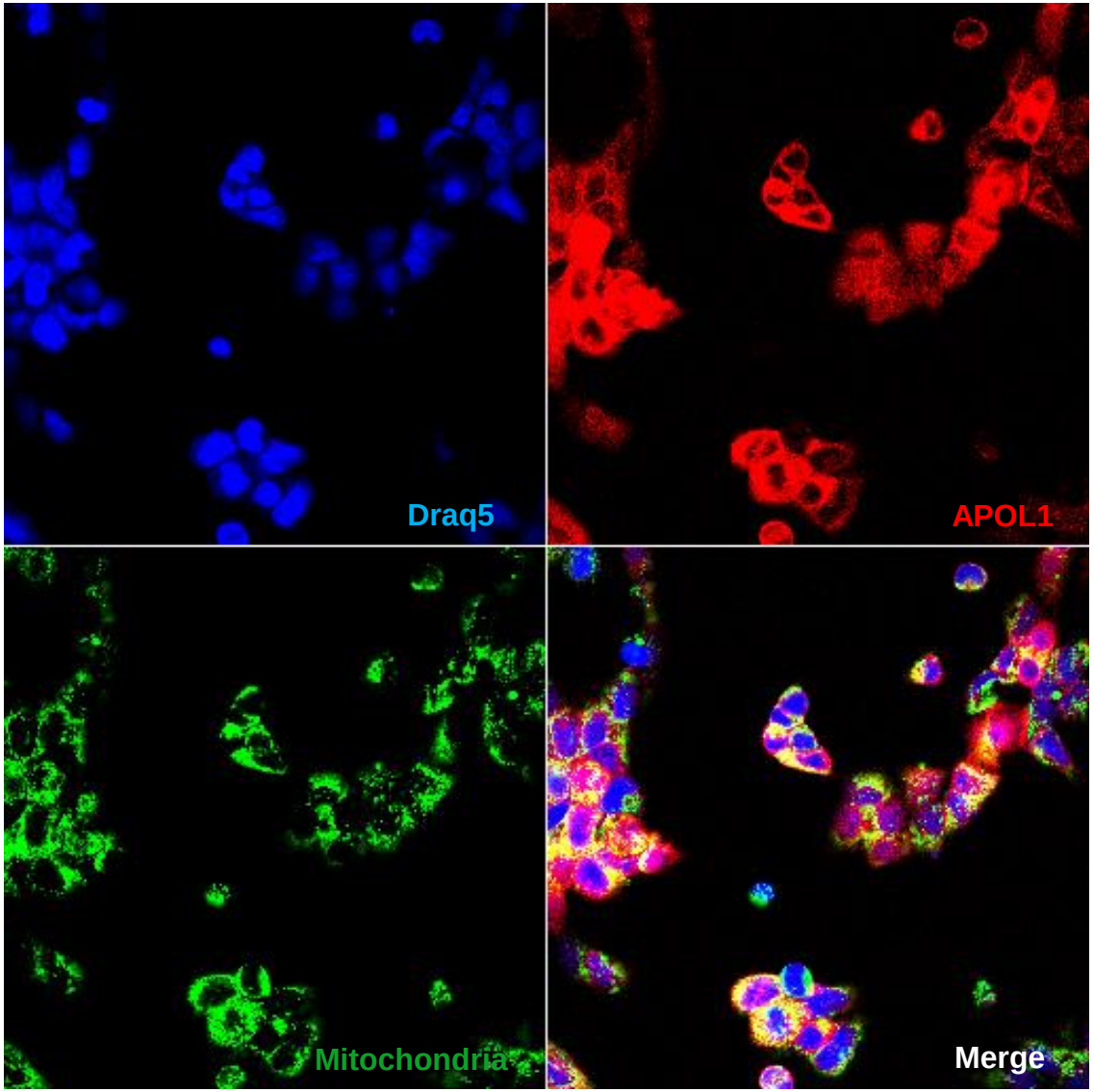

Supplemental Figure 9A

Supplemental Figure 9. APOL1 co-localizes with mitochondria.
A) Confocal immunofluorescence microscopy (630x) on HEK293 Tet-on G0 cells with Dox induction as representative of APOL1 colocalization with mitochondria. After fixation with 4% paraformadehyde and washing with PBS, cells were stained for APOL1 (red), ATP synthase 5A1 (ATP5A1; green), a mitochondria marker, and Draq5 (blue), a nuclear stain.

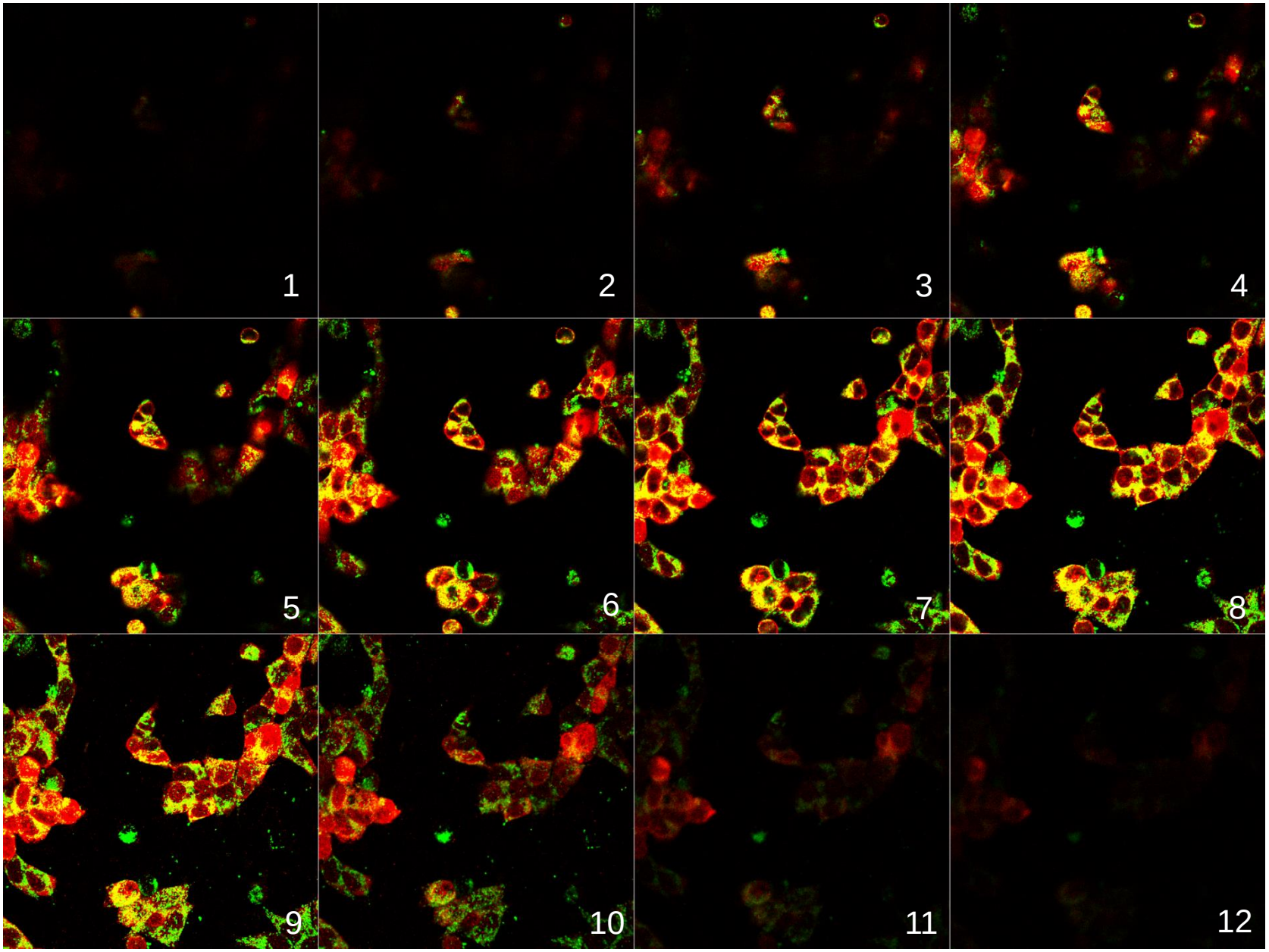

Supplemental Figure 9B

Supplemental Figure 9. APOL1 co-localizes with mitochondria.
B) Confocal immunofluorescence microscopy (630x) reveals the photo gallery of HEK293 Tet-on G0 with Dox induction as representative of APOL1 co-localization with mitochondria. To sufficiently display the location of APOL1 and mitochondria, only the fluorescent signals of APOL1 (red) and ATP synthase 5A1 (ATP5A1; green), a mitochondria marker, are shown in the serial photo gallery (1-12) for the z-stack model (1μm depth for each scan). Fluorescent signals for APOL1 (red) are present in mitochondria (green) and beyond.

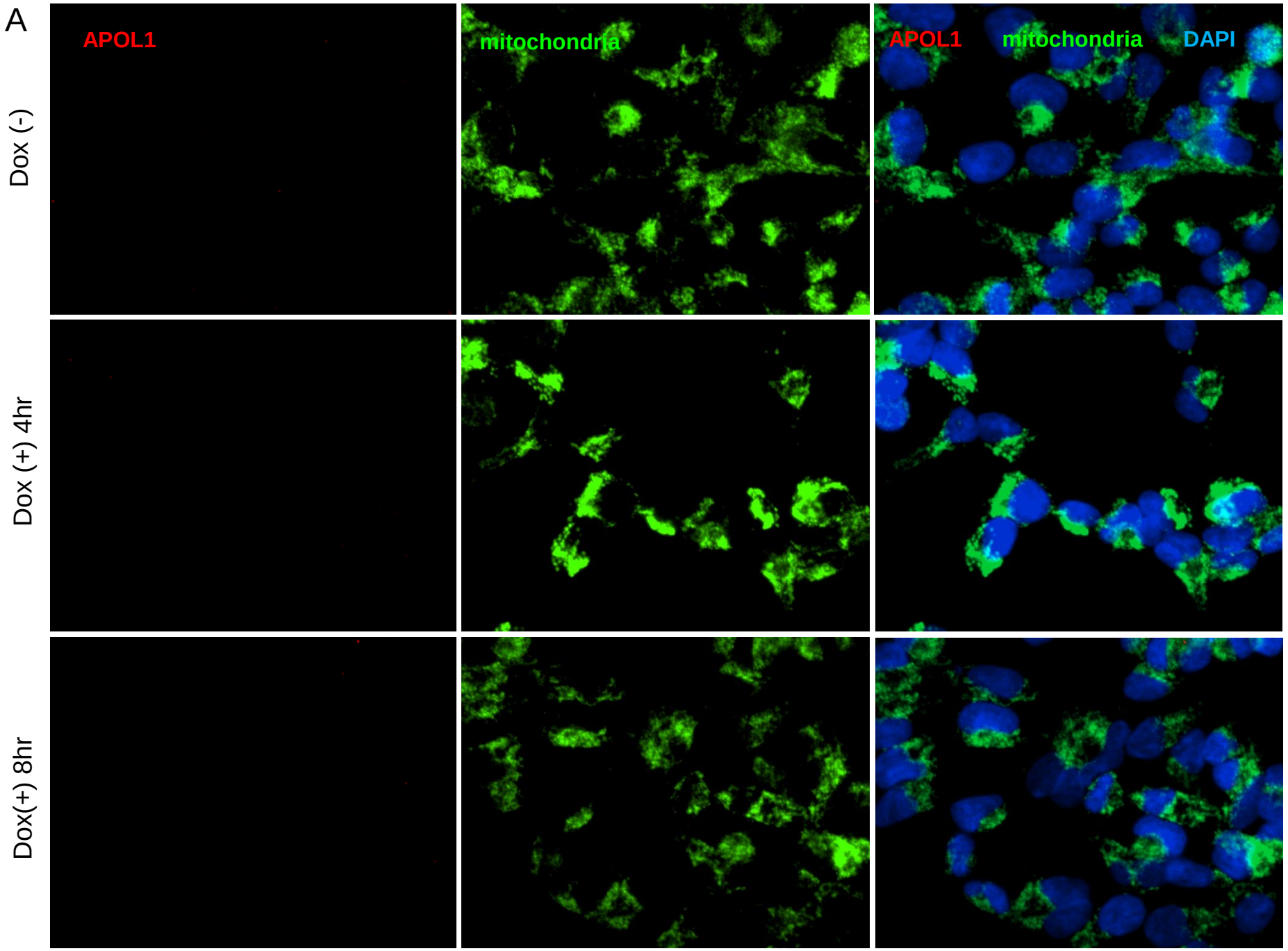

Supplemental Figure 10

HEK293 Tet-on EV cells

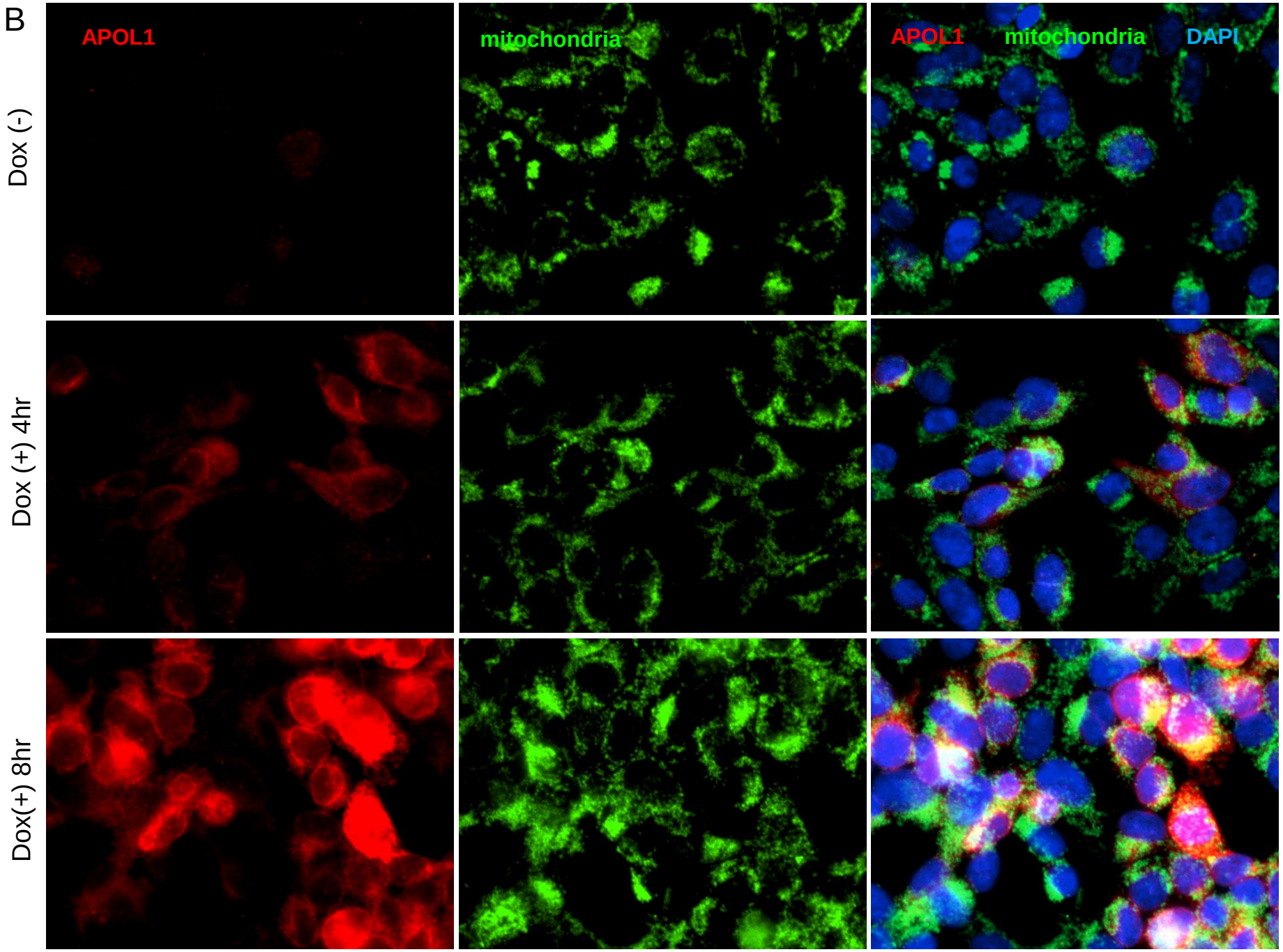

Supplemental Figure 10

HEK293 Tet-on G0 cells

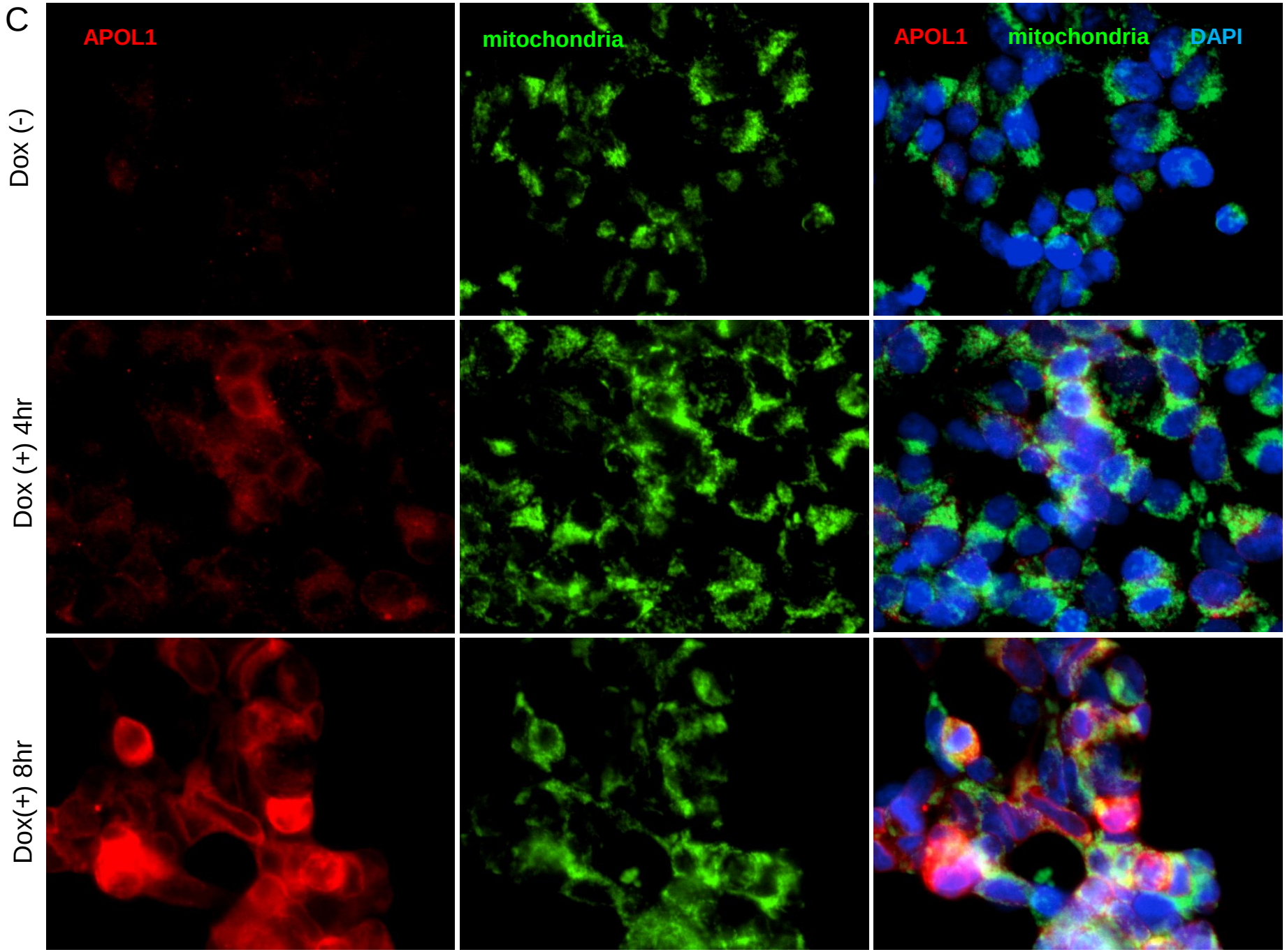

Supplemental Figure 10

HEK293 Tet-on G1 cells

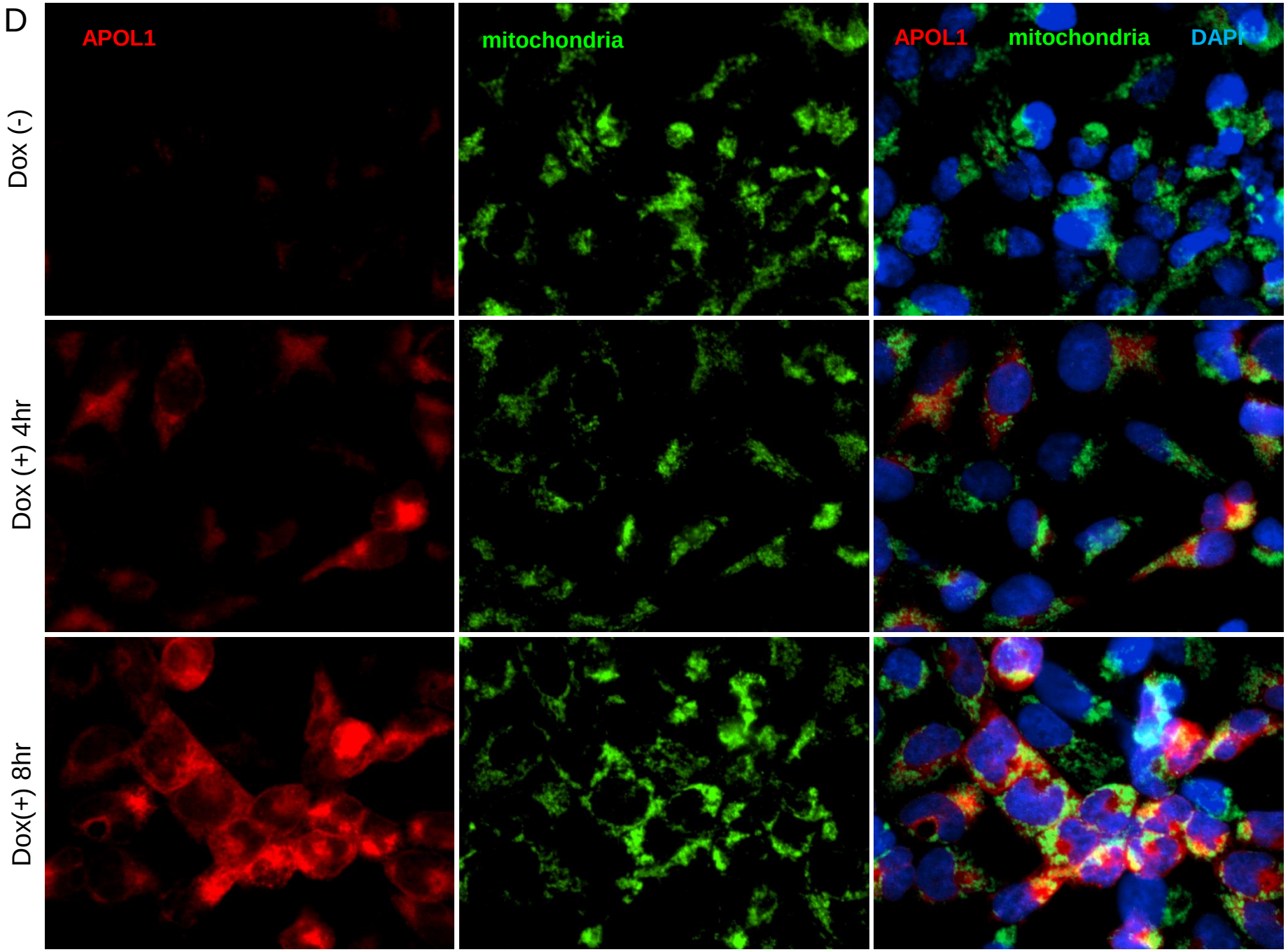

Supplemental Figure 10

HEK293 Tet-on G2 cells

Supplemental Figure 10. APOL1 co-localizes with mitochondria in HEK293 Tet-on *APOL1* G0, G1 and G2 cells with Dox induction

HEK293 Tet-on empty vector (EV), G0, G1 and G2 cells (panels A, B, C, and D respectively) in the absence of Dox and after 4hr or 8hr Dox induction were washed with PBS and fixed with 4% paraformaldehyde. Cells were stained for APOL1 (red) with Epitomics anti-APOL1 antibody, mitochondria (green) with ATP synthase 5 A1 (ATP5A1) antibody and counterstained with nuclear dye DAPI (blue). No APOL1 was present in empty vector cells with (+) or without (-) Dox induction. Trace amounts of APOL1 were present in G0, G1 and G2 cells without (-) Dox induction; elevated APOL1 was observed in G0, G1 and G2 cells with (+) Dox induction for 4 hr; substantially elevated APOL1 was observed in G0, G1 and G2 cells with (+) Dox induction for 8 hr.

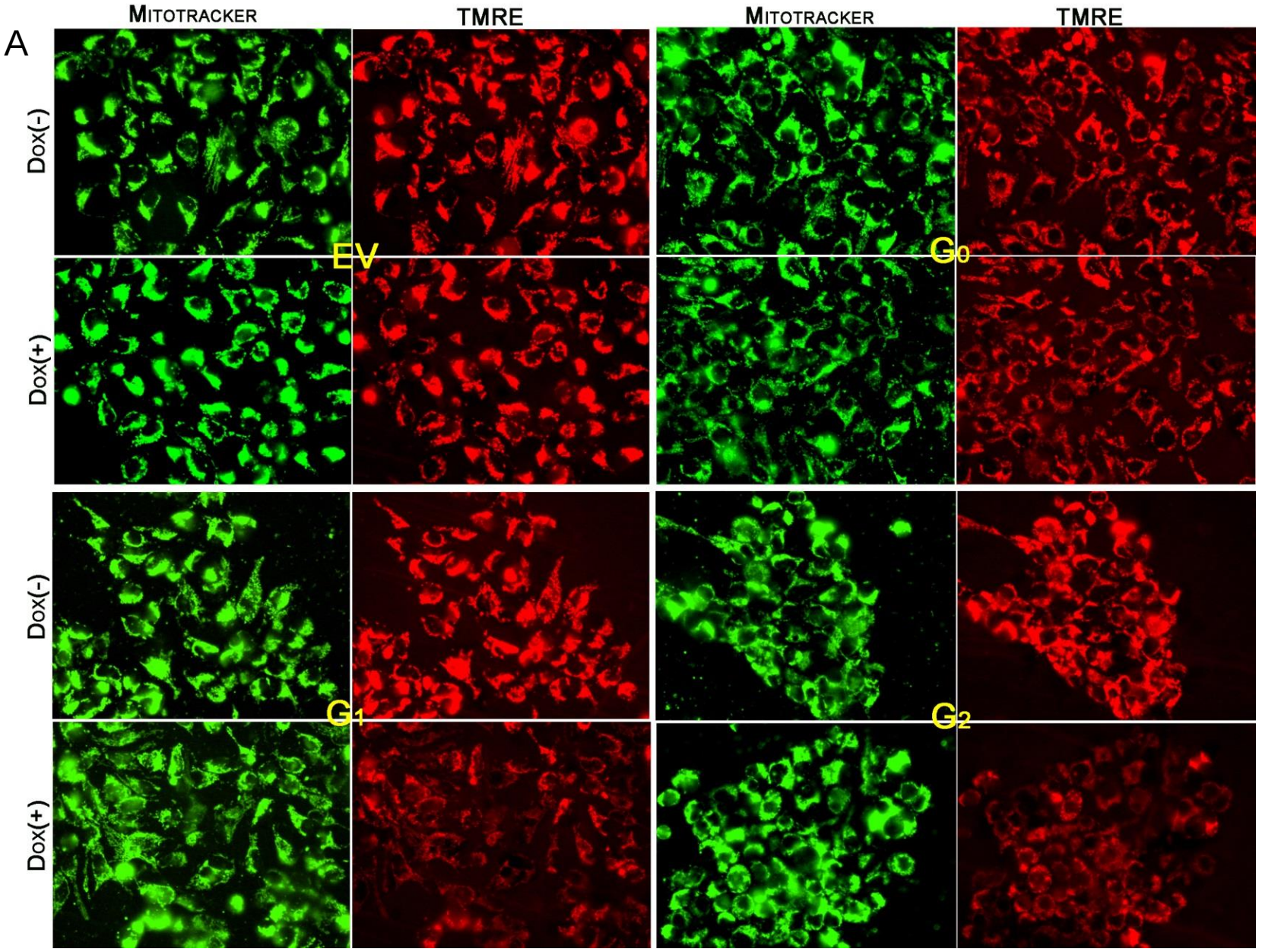

Supplemental
Figure 11

Supplemental Figure 11. Mitochondrial membrane potential is reduced in Dox-reduced HEK293 Tet-on *APOL1* G1 and G2 cells.
A) HEK293 Tet-on cells stably expressing *APOL1* G0, G1, or G2 were grown with (+) or without (-) Dox for 7.5 hr in full DMEM media. Cells were subsequently incubated for 30 min with a final concentration of 50 nM mitotracker green (Invitrogen) and 10 nM TMRE (Tetramethylrhodamine ethyl ester, Invitrogen), a live cell fluorescence marker of mitochondrial membrane potential. Mitochondrial mass did not differ across HEK293 Tet-on *APOL1* cells (+/-) Dox induction, indicated by constant mitochondrial green signals. However, HEK293 Tet-on G1 and G2 cells appeared to lose mitochondrial membrane potential when induced by Dox.

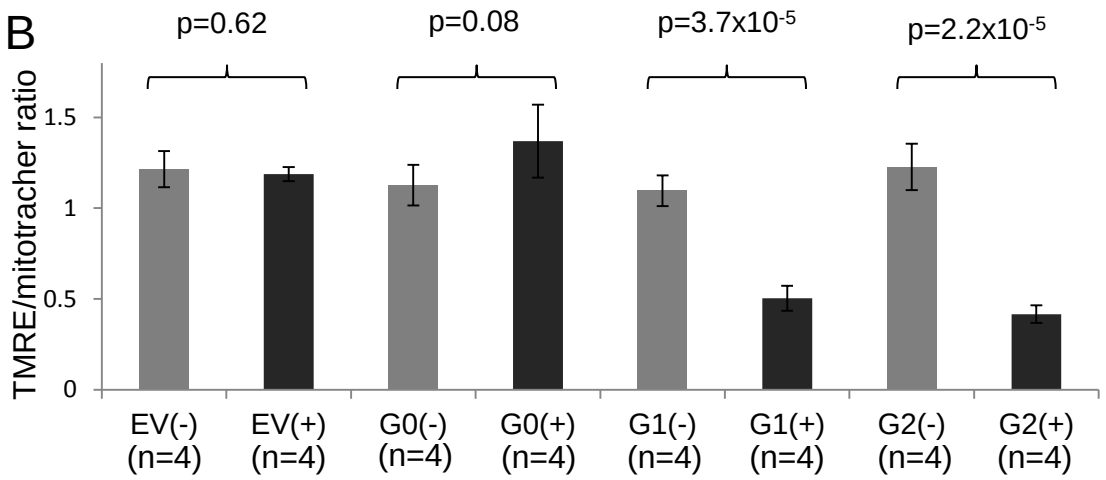

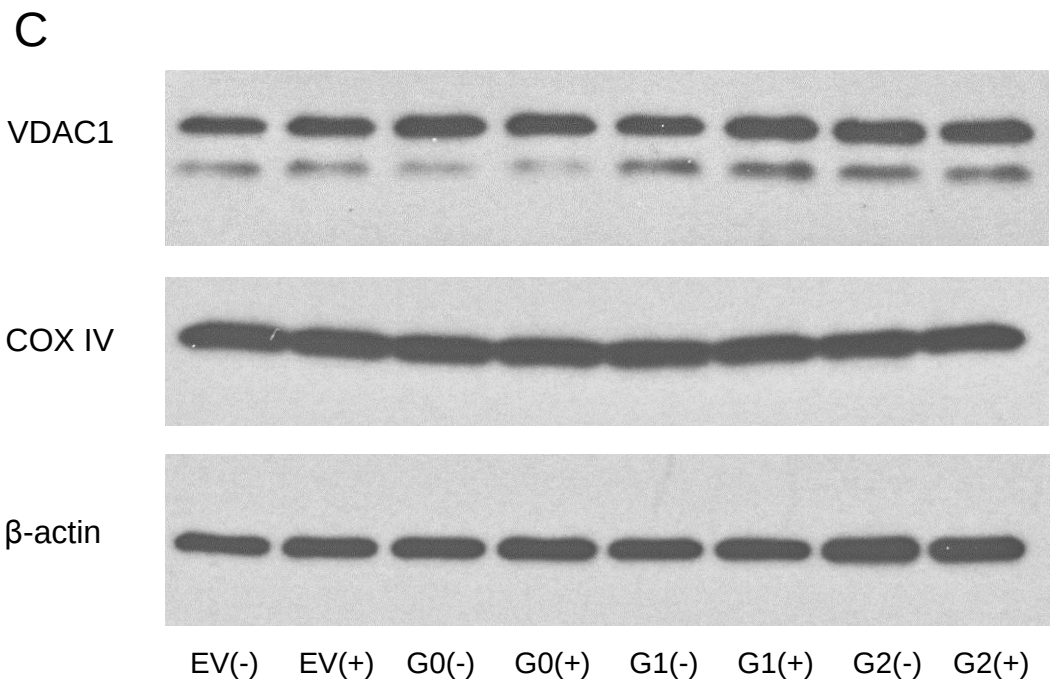

Supplemental Figure 11

Supplemental Figure 11. Mitochondrial membrane potential is reduced in Dox-reduced HEK293 Tet-on *APOL1* G1 and G2 cells.

B) Reduced fluorescence signal ratio of mitochondrial membrane potential (TMRE) and mitotracker green in HEK293 Tet-on G1 and G2 cells with Dox induction. Fluorescence signals of TMRE and mitotracker green were captured using an Olympus IX71 fluorescence microscope on four different fields/groups of each type of HEK293 Tet-on cells of *APOL1* genotype (+/-) Dox induction. Fluorescence signals were measured by Image J (http://imagej.nih.gov/ij/). A paired t-test was used to estimate the TMRE/mitoctracker ratio difference for cells with (+) and without (-) Dox induction after correction for non-specific background.

C) Mitochondrial protein expression remains constant in HEK293 Tet-on cells with and without Dox induction. Stabilized HEK293 Tet-on cells grown with (+) or without (-) Dox were lysed and fractionated by SDS-PAGE, then probed with antibodies for mitochondrial proteins COXIV and porin/VDAC1. *APOL1* G1 and G2 renal-risk variants did not alter mitochondrial mass, relative to G0 (reference), with or without Dox induction.

EV: HEK293 Tet-on cell line with empty pTRE2hyg plasmid.

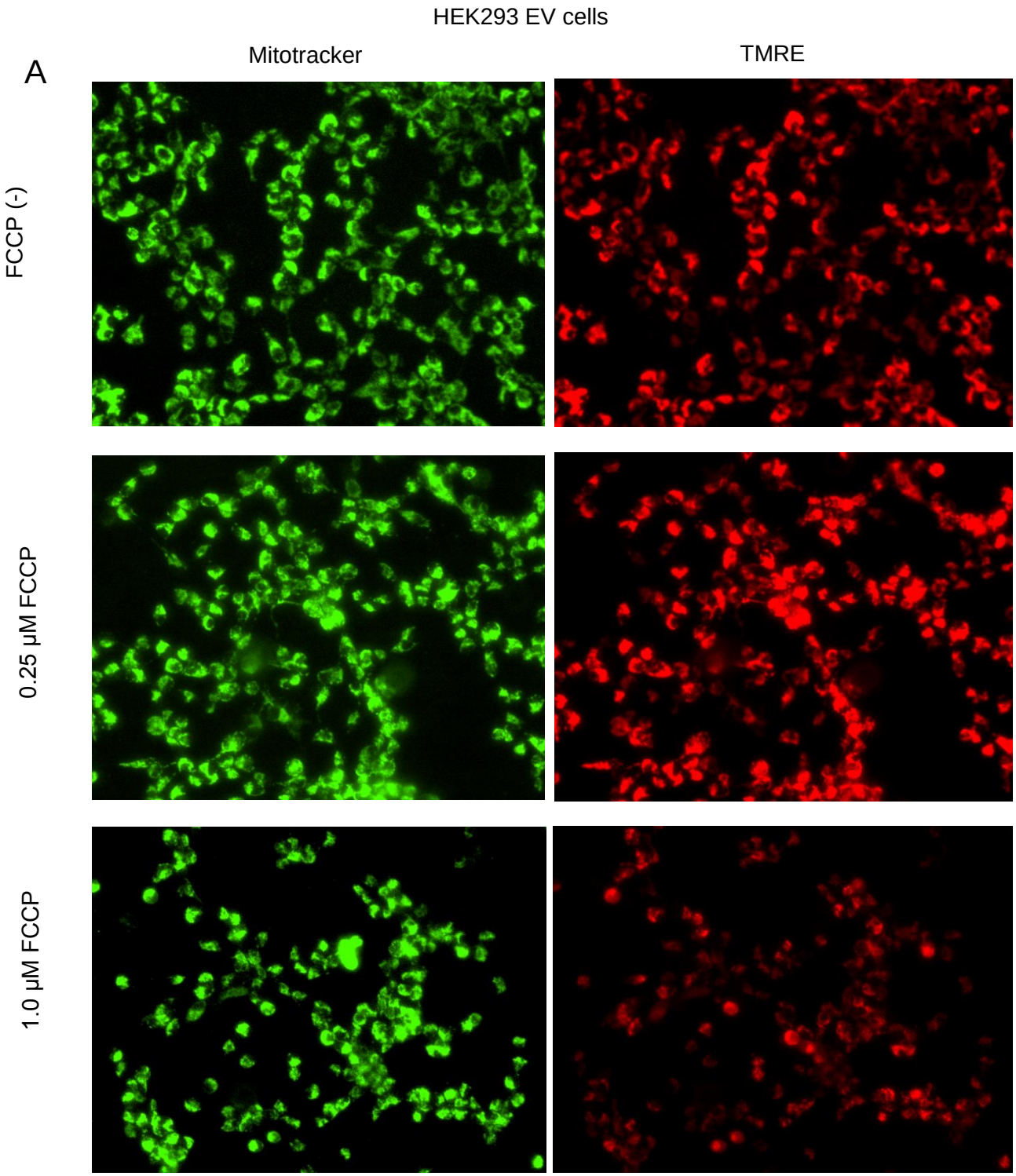

Supplemental
Figure 12

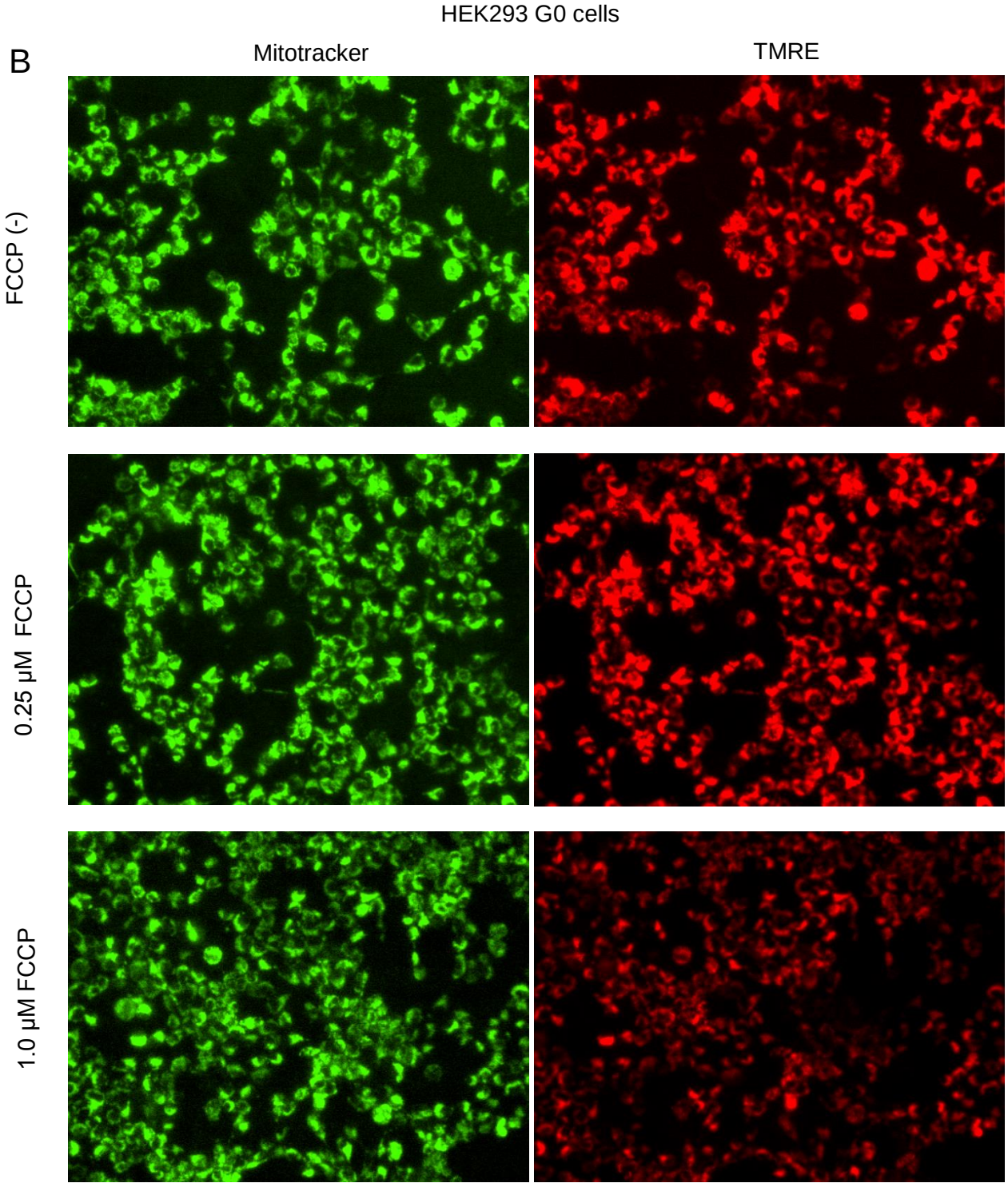

Supplemental
Figure 12

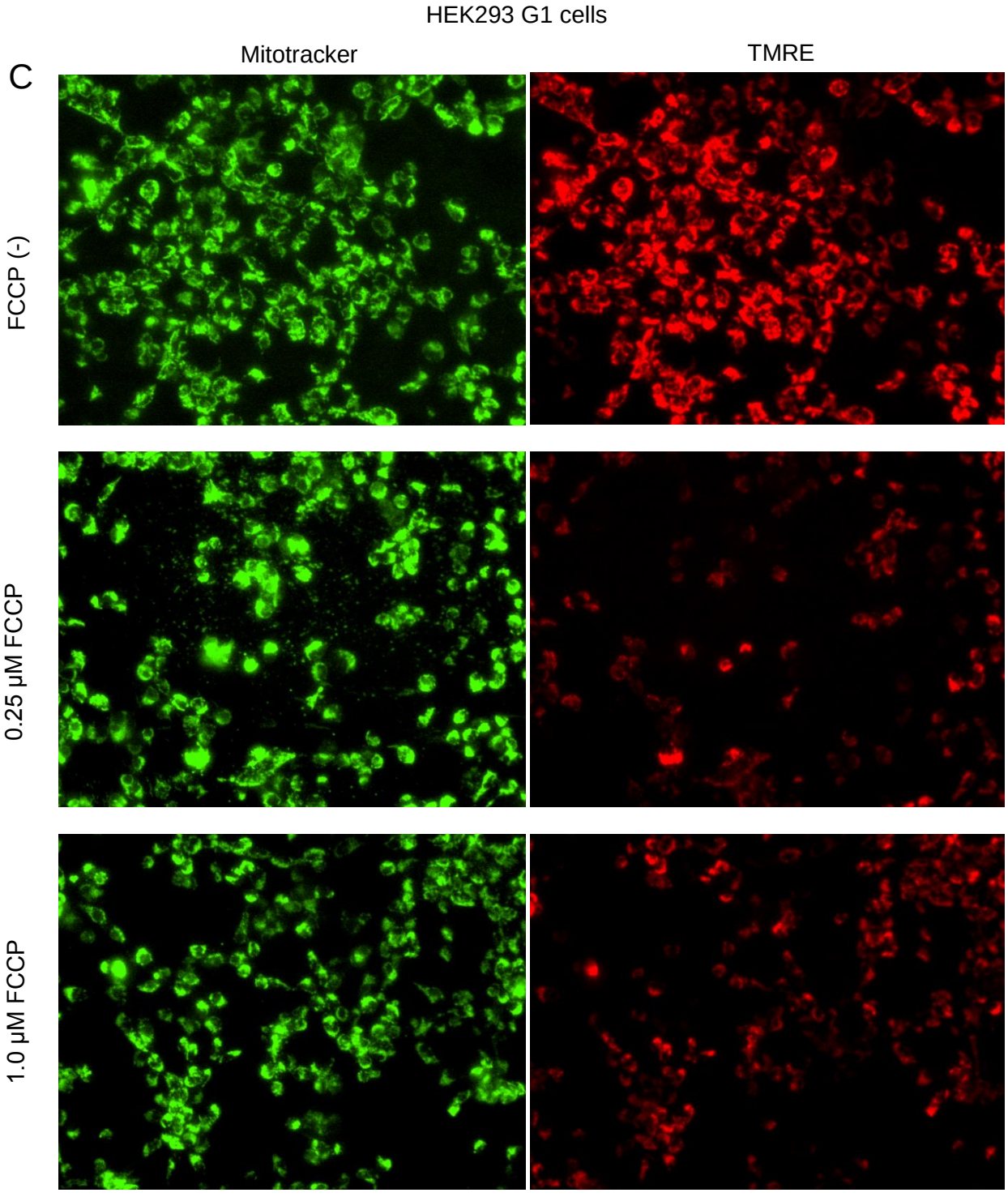

Supplemental
Figure 12

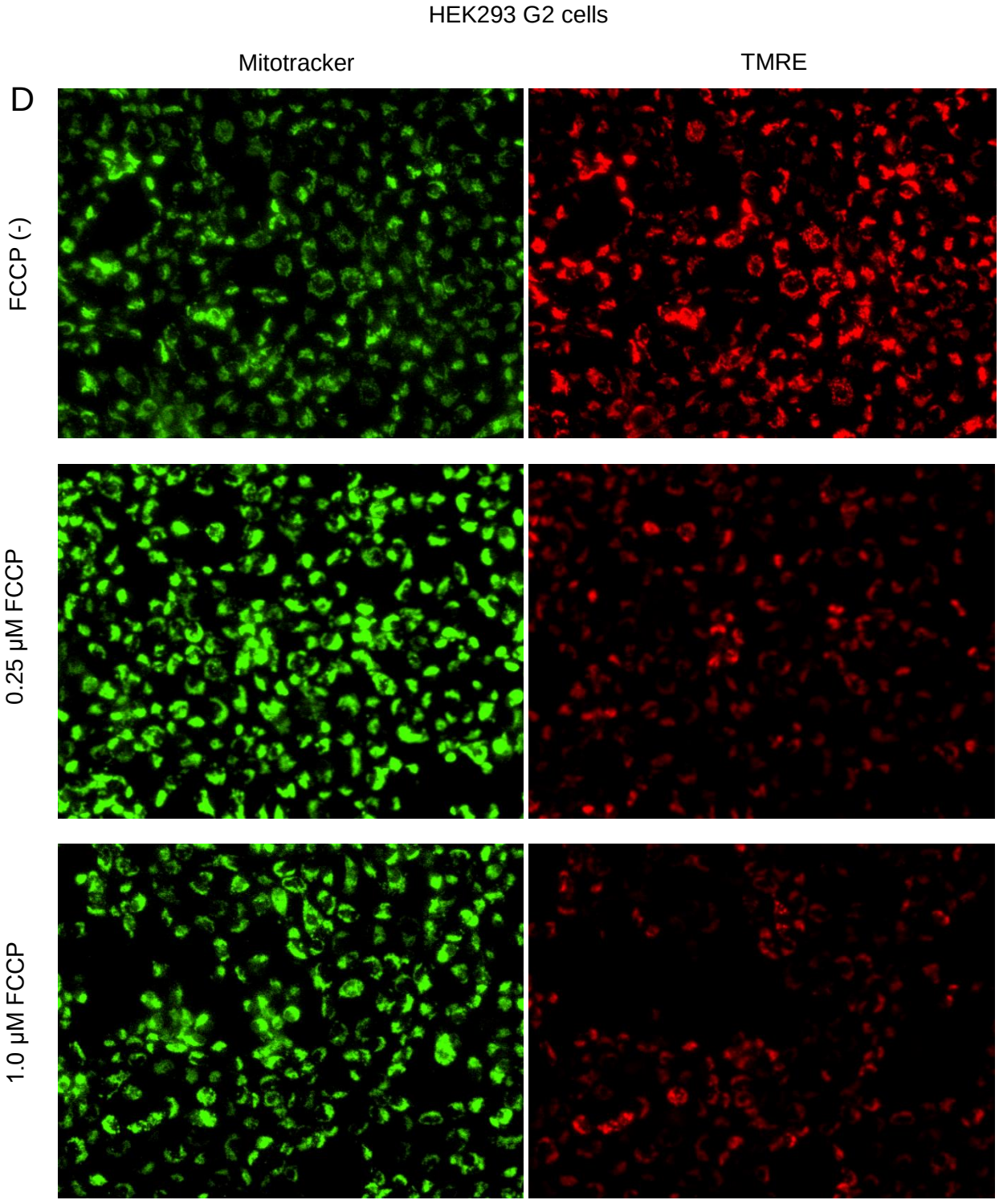

Supplemental
Figure 12

Supplemental Figure 12. Mitochondrial membrane potential declines in HEK293 Tet-on cells with FCCP incubation

Non-induced HEK293 Tet-on empty vector (EV), G0, G1 and G2 cells (panels A, B, C and D, respectively) were incubated for 30 min with a final concentration of 50 nM mitotracker green (Invitrogen) and 10 nM TMRE (Tetramethylrhodamine ethyl ester, Invitrogen), a live cell fluorescence marker of mitochondrial membrane potential, on a 96-well cell culture plate. FCCP was subsequently added to culture media in final concentrations of 0.25 µM and 1.0 µM for 30 minutes, respectively, in cells of different genotypes together with FCCP-free cells as controls. Cell images were captured by an Olympus IX71 fluorescence microscope. The mitochondrial membrane potential remained virtually intact for EV and G0 cells treated with 0.25 µM FCCP; however, reduced mitochondrial membrane potential was observed in G1 and G2 cells treated with 0.25 µM FCCP. When EV, G0, G1 and G2 cells were treated with 1.0 µM FCCP, all types cells appeared to display reduced mitochondrial membrane potential.

Supplemental Video

Supplemental Video 1. Co-localization of APOL1 with mitochondria in Dox-induced HEK293 Tet-on G0 cells as assessed by confocal microscopy images (z-stack model). Serial confocal immunofluorescence microscopy (630x) was performed to form the animated video of 1 μm depth per scan for HEK293 Tet-on G0 wells, as representative of all HEK293 *APOL1* cells with Dox induction for 8 hr. After washing with PBS, cells were stained for APOL1 (red), mitochondria (ATP5A1; green), corresponding to Supplemental Figure 9.

Supplemental Table 1. Top 20 pathways revealed from most differentially expressed 1056 genes by Dox-induced *APOL1* over-expression in the HEK293 G0 Tet-on cell line using Cytoscape BiNGO

GO-ID	Description	x	n	X	N	p-value	FDR p-value
43231	intracellular membrane-bounded organelle	539	8338	901	17758	1.26E-15	3.72E-12
43227	membrane-bounded organelle	539	8345	901	17758	1.54E-15	3.72E-12
5634	nucleus	349	5181	901	17758	1.66E-10	1.80E-07
3676	nucleic acid binding	240	3254	901	17758	1.66E-10	1.80E-07
44424	intracellular part	643	10939	901	17758	1.86E-10	1.80E-07
34641	cellular nitrogen compound metabolic process	168	2080	901	17758	3.30E-10	2.66E-07
5622	intracellular	656	11291	901	17758	1.04E-09	7.20E-07
44237	cellular metabolic process	334	4990	901	17758	1.28E-09	7.72E-07
44260	cellular macromolecule metabolic process	250	3511	901	17758	1.95E-09	1.05E-06
43226	organelle	558	9327	901	17758	3.25E-09	1.54E-06
43229	intracellular organelle	557	9313	901	17758	3.69E-09	1.54E-06
6807	nitrogen compound metabolic process	171	2198	901	17758	3.82E-09	1.54E-06
33554	cellular response to stress	66	622	901	17758	1.04E-08	3.86E-06
44238	primary metabolic process	344	5287	901	17758	1.80E-08	5.94E-06
3677	DNA binding	176	2329	901	17758	1.84E-08	5.94E-06
90304	nucleic acid metabolic process	122	1464	901	17758	2.39E-08	7.23E-06
8152	metabolic process	379	5955	901	17758	2.63E-08	7.49E-06
44238	primary metabolic process	344	5287	901	17758	1.80E-08	5.94E-06
3677	DNA binding	176	2329	901	17758	1.84E-08	5.94E-06
90304	nucleic acid metabolic process	122	1464	901	17758	2.39E-08	7.23E-06

Note: x, number of gene IDs identified in the designated pathway among input gene IDs; X, number of input gene IDs selected by BiNGO; n, number of known gene IDs in the designated pathway; N, number of background gene IDs selected from the GO pool by BiNGO. Replicated pathways in the subsequent Ingenuity pathway analysis are shown in red. P values are shown as scientific E notation (e.g. 2.00E-5 is equivalent to 2.00×10^{-5}) hereafter throughout the supplemental tables.

Supplemental Table 2. Top canonical pathways detected based on the most differentially expressed genes by Dox-induced *APOL1* over-expression (HEK293 G0 Tet-on cell line using Ingenuity pathway analysis)

Ingenuity Canonical Pathways	p-value	Molecules
Unfolded protein response	9.05E-07	MAP2K7,HSPA14,DDIT3,INSIG1,XBP1,CEBPB,DNAJB9,HSPA5,CEBPG,BCL2,SEL1L,EDEM1,ERO1LB
ERK5 Signaling	1.50E-04	MYC,FOS,SGK1,MEF2D,GNA12,MAP3K8,RPS6KA1,RPS6KA2,CREB3L4,ATF2,MAP3K2
NRF2-mediated Oxidative Stress Response	3.13E-04	MAP2K7,MAPK1,PPIB,DNAJC19,MAF,HSPB8,HERPUD1,DNAJC10,DNAJB9,MAFF,BACH1,MAFG,FOS,AKR1A1,SOD2,JUN,MAP2K3,GSK3B,UBE2E3,DNAJB6
p38 MAPK Signaling	3.77E-04	ATF1,DDIT3,SRF,CREB3L4,MAPK12,ATF2,MYC,DUSP1,MEF2D,DUSP10,MAP2K3,RPS6KA2,EEF2K,RPS6KA1,TAB1
tRNA Charging	3.82E-04	WARS,CARS,GARS,EARS2,AARS,SARS,IARS,EPRS

Replicated pathways in the prior BiNGO pathway analysis (Table S1) are shown in red.

Supplemental Table 3. Top five upstream regulators detected based on the most differentially expressed genes by Dox-induced *APOL1* over-expression (HEK293 G0 Tet-on cell line using Ingenuity Pathway Analysis)

Upstream Regulator	Predicted Activation State	Activation z-score	p-value	Target molecules in dataset
ATF4	Inhibited	-3.56	4.53E-20	AARS,ASNS,BCAT1,CEBPB,CEBPG,CHAC1,CTH,DDIT3,DDIT4,EIF2S2,EIF4EBP1,GARS,GDF15,HERPUD1,HSPA5,IGFBP5,JUN,KLF4,MTHFD2,PCK2,PSAT1,PSPH,PYCR1,SARS,SEL1L,SHMT2,SIGMAR1,SLC38A2,SLC3A2,SLC6A9,SLC7A5,STC2,TNFRSF12A,TRIB3,WARS,XPOT,
tosedostat	Inhibited	-3.184	7.46E-16	ASNS,ASS1,CARS,CBS/LOC102724560,CEBPB,CHAC1,CTH,CXCL8,DDIT3,DDIT4,PSAT1,SARS,SLC38A2,SLC7A11,STC2,TRIB3,WARS,
TRIB3	Activated	3.346	1.18E-14	ASNS,CDC25A,CTH,DDIT3,DDIT4,GARS,GDF15,HERPUD1,ID1,MTHFD2,PCK2,PSAT1,PSPH,STC2,TRIB3,
tunicamycin	Inhibited	-3.464	6.04E-14	ASNS,ATP2A2,CCND1,CEBPB,CPT2,CREB3L2,DDIT3,DDIT4,DNAJB9,EDEM1,EDEM2,EGR1,ERO1LB,GADD45B,GPT2,HERPUD1,HSPA5,KLF4,LONP1,MANF,MTDH,MYC,NFKBIA,PCK2,PDIA6,PLIN2,SDF2L1,SEL1L,SIGMAR1,SLC7A11,WFS1,XBP1,
XBP1	Inhibited	-4.709	1.25E-12	ATP2A2,BCL2,BET1,COPG1,CRK,CXCL8,DDIT3,DNAJB9,DNAJC10,EDEM1,EDEM2,ERO1LB,FKBP11,FKBP14,FKBP2,GOSR2,HERPUD1,HSPA5,HYOU1,KDELR3,KLF4,MYC,PDIA4,PDIA6,PPIB,SDF2L1,SEC11C,SEC23B,SEC24D,SEC63,SERP1,SPCS3,SSR1,STX5,TXNDC5,WFS1,

Related regulators of the ER stress pathway detected in the prior analyses (Supplemental Table 1 & 2), are shown in red. |Activation Z score|>3.

Supplemental Table 4. Top pathways revealed from most differentially expressed genes by Dox-induced *APOL1* in the HEK293 G1 Tet-on cell line using Cytoscape BiNGO

GO-ID	Description	x	n	X	N	p-value	FDR p-value
	Top 20 significant pathways enriched in 1357 qualified transcripts						
5634	nucleus	475	5183	1140	17760	1.00E-20	5.49E-17
43231	intracellular membrane-bounded organelle	677	8338	1140	17760	2.19E-18	5.07E-15
43227	membrane-bounded organelle	677	8345	1140	17760	2.78E-18	5.07E-15
3676	nucleic acid binding	321	3253	1140	17760	2.42E-17	3.30E-14
44424	intracellular part	829	10941	1140	17760	2.34E-16	2.55E-13
5622	intracellular	848	11293	1140	17760	6.45E-16	5.87E-13
30528	transcription regulator activity	175	1507	1140	17760	2.50E-15	1.96E-12
10556	regulation of macromolecule biosynthetic process	283	2874	1140	17760	5.93E-15	4.05E-12
60255	regulation of macromolecule metabolic process	318	3374	1140	17760	2.63E-14	1.60E-11
6357	regulation of transcription from RNA polymerase II promoter	104	747	1140	17760	3.57E-14	1.95E-11
10468	regulation of gene expression	283	2925	1140	17760	5.55E-14	2.59E-11
31323	regulation of cellular metabolic process	343	3733	1140	17760	5.69E-14	2.59E-11
34641	cellular nitrogen compound metabolic process	217	2082	1140	17760	8.30E-14	3.49E-11
3677	DNA binding	235	2328	1140	17760	1.93E-13	7.52E-11
80090	regulation of primary metabolic process	326	3551	1140	17760	3.88E-13	1.41E-10
45449	regulation of transcription	256	2619	1140	17760	4.54E-13	1.46E-10
9889	regulation of biosynthetic process	288	3042	1140	17760	4.55E-13	1.46E-10
19222	regulation of metabolic process	352	3916	1140	17760	5.14E-13	1.56E-10
44237	cellular metabolic process	428	4989	1140	17760	5.49E-13	1.58E-10
43233	organelle lumen	181	1680	1140	17760	8.59E-13	2.26E-10
	Top 10 significant pathways enriched in 695 qualified transcripts down-regulated by G1 over-expression						
5739	mitochondrion	95	1270	579	17779	1.24E-14	4.07E-11
34641	cellular nitrogen compound metabolic process	121	2081	579	17779	9.22E-11	1.51E-07
8152	metabolic process	266	5957	579	17779	1.94E-10	2.12E-07

6807	nitrogen compound metabolic process	123	2199	579	17779	7.29E-10	5.98E-07
44237	cellular metabolic process	229	4990	579	17779	9.15E-10	6.00E-07
48037	cofactor binding	29	253	579	17779	4.23E-09	2.31E-06
3824	catalytic activity	227	5093	579	17779	1.80E-08	8.44E-06
9058	biosynthetic process	100	1797	579	17779	5.41E-08	2.22E-05
42180	cellular ketone metabolic process	44	577	579	17779	1.57E-07	5.72E-05
44238	primary metabolic process	229	5288	579	17779	1.92E-07	5.72E-05
43436	oxoacid metabolic process	43	563	579	17779	2.09E-07	5.72E-05
19752	carboxylic acid metabolic process	43	563	579	17779	2.09E-07	5.72E-05
6082	organic acid metabolic process	43	570	579	17779	2.94E-07	7.41E-05
	Top 10 significant pathways enriched in 662 qualified transcripts up-regulated by G1 over-expression						
31323	regulation of cellular metabolic process	253	3731	563	17771	1.99E-38	6.58E-35
10556	regulation of macromolecule biosynthetic process	216	2872	563	17771	3.13E-38	6.58E-35
5634	nucleus	307	5180	563	17771	1.81E-37	2.54E-34
19222	regulation of metabolic process	258	3914	563	17771	3.31E-37	3.48E-34
10468	regulation of gene expression	216	2923	563	17771	4.92E-37	4.02E-34
9889	regulation of biosynthetic process	221	3040	563	17771	5.73E-37	4.02E-34
60255	regulation of macromolecule metabolic process	235	3372	563	17771	7.44E-37	4.34E-34
30528	transcription regulator activity	147	1506	563	17771	8.26E-37	4.34E-34
31326	regulation of cellular biosynthetic process	218	3016	563	17771	5.88E-36	2.75E-33
45449	regulation of transcription	198	2618	563	17771	9.57E-35	4.03E-32

Note: x, number of gene IDs identified in the designated pathway among input gene IDs; X, number of input gene IDs selected by BiNGO; n, number of known gene IDs in the designated pathway; N, number of background gene IDs selected from the GO pool by BiNGO. Replicated pathways in the subsequent pattern-based analyses are shown in red.

Supplemental Table 5. Top pathways revealed from most differentially expressed genes by Dox-induced *APOL1* in the HEK293 G2 Tet-on cell line using Cytoscape BiNGO

GO-ID	Description	x	n	X	N	p-value	FDR p-value
	Top 20 significant pathways enriched in 2409 qualified transcripts						
43227	membrane-bounded organelle	1240	8327	2022	17725	3.64E-43	2.45E-39
43231	intracellular membrane-bounded organelle	1238	8320	2022	17725	8.05E-43	2.71E-39
44424	intracellular part	1495	10915	2022	17725	1.26E-35	2.84E-32
5622	intracellular	1529	11268	2022	17725	7.46E-35	1.26E-31
5634	nucleus	826	5170	2022	17725	4.44E-33	5.98E-30
43229	intracellular organelle	1295	9289	2022	17725	2.21E-29	2.48E-26
43226	organelle	1296	9303	2022	17725	2.99E-29	2.88E-26
44237	cellular metabolic process	775	4985	2022	17725	2.93E-26	2.47E-23
44260	cellular macromolecule metabolic process	577	3509	2022	17725	5.16E-24	3.86E-21
34641	cellular nitrogen compound metabolic process	381	2081	2022	17725	2.56E-23	1.72E-20
8152	metabolic process	873	5947	2022	17725	6.38E-22	3.90E-19
6807	nitrogen compound metabolic process	390	2199	2022	17725	2.92E-21	1.64E-18
90304	nucleic acid metabolic process	285	1464	2022	17725	3.61E-21	1.87E-18
6139	nucleobase, nucleoside, nucleotide and nucleic acid metabolic process	329	1790	2022	17725	2.89E-20	1.39E-17
70013	intracellular organelle lumen	307	1642	2022	17725	5.08E-20	2.28E-17
31974	membrane-enclosed lumen	317	1713	2022	17725	5.65E-20	2.38E-17
43233	organelle lumen	310	1677	2022	17725	1.89E-19	7.50E-17
5737	cytoplasm	1056	7636	2022	17725	1.01E-18	3.77E-16
44238	primary metabolic process	775	5280	2022	17725	1.41E-18	4.99E-16
3676	nucleic acid binding	513	3247	2022	17725	2.96E-17	9.97E-15
	Top 10 significant pathways enriched in 1414 qualified transcripts down-regulated by G2 over-expression						
5739	mitochondrion	168	1270	1169	17765	4.03E-19	1.88E-15
48037	cofactor binding	58	253	1169	17765	2.48E-17	5.76E-14
44444	cytoplasmic part	457	5139	1169	17765	7.21E-15	1.05E-11

8152	metabolic process	514	5952	1169	17765	9.02E-15	1.05E-11
55114	oxidation reduction	96	647	1169	17765	3.28E-14	3.05E-11
50662	coenzyme binding	43	181	1169	17765	9.13E-14	7.08E-11
44237	cellular metabolic process	440	4987	1169	17765	1.42E-13	9.42E-11
34641	cellular nitrogen compound metabolic process	218	2079	1169	17765	5.25E-13	3.05E-10
43231	intracellular membrane-bounded organelle	666	8336	1169	17765	6.84E-13	3.54E-10
43227	membrane-bounded organelle	666	8343	1169	17765	8.37E-13	3.89E-10
	Top 10 significant pathways enriched in 995 qualified transcripts up-regulated by G2 over-expression						
5634	nucleus	480	5169	860	17741	5.54E-63	2.77E-59
31323	regulation of cellular metabolic process	362	3729	860	17741	1.03E-46	2.57E-43
19222	regulation of metabolic process	371	3910	860	17741	9.14E-46	1.52E-42
10468	regulation of gene expression	302	2919	860	17741	1.09E-42	1.36E-39
10556	regulation of macromolecule biosynthetic process	298	2869	860	17741	2.37E-42	2.10E-39
60255	regulation of macromolecule metabolic process	330	3368	860	17741	2.52E-42	2.10E-39
9889	regulation of biosynthetic process	304	3036	860	17741	4.18E-40	2.99E-37
80090	regulation of primary metabolic process	335	3546	860	17741	1.27E-39	7.93E-37
31326	regulation of cellular biosynthetic process	301	3013	860	17741	2.04E-39	1.13E-36
30528	transcription regulator activity	195	1505	860	17741	3.58E-39	1.79E-36

Note: x, number of gene IDs identified in the designated pathway among input gene IDs; X, number of input gene IDs selected by BiNGO; n, number of known gene IDs in the designated pathway; N, number of background gene IDs selected from the GO pool by BiNGO. Replicated pathways in the subsequent pattern-based analyses are shown in red.

Supplemental Table 6. Top pathways detected from the most differentially expressed genes with Dox-induced *APOL1* G1 vs. G0 (HEK293 Tet-on cell lines based on human Illumina HT-12 v4 arrays using Cytoscape BiNGO)

GO-ID	Description	x	n	X	N	p-value	FDR p-value
	Top pathway enriched in 293 qualified transcripts						
6259	DNA metabolic process	19	516	211	17787	1.32E-05	2.07E-02
	Top pathway enriched in 70 qualified transcripts down-regulated by G1						
5739	mitochondrion	14	1271	61	17788	7.87E-05	4.43E-02
	Pathway enriched in 223 qualified transcripts up-regulated by G1						
	None						

Note: x, number of gene IDs identified in the designated pathway among input gene IDs; X, number of input gene IDs selected by BiNGO; n, number of known gene IDs in the designated pathway; N, number of background gene IDs selected from the GO pool by BiNGO. Replicated pathways in the subsequent Ingenuity pathway analysis are shown in red. Since no pathway reached the nominal significance for FDR p<0.01, only the top one with FDR p<0.05 is presented. Replicated pathway(s) in the subsequent pattern-based analyses are shown in red.

Supplemental Table 7. Top pathways detected from the most differentially expressed genes with Dox-induced *APOL1* G2 vs. G0 (HEK293 Tet-on cell lines based on human Illumina HT-12 v4 arrays using Cytoscape BiNGO)

GO-ID	Description	x	n	X	N	p-value	FDR p-value
	Significant pathways enriched in 609 qualified transcripts						
43231	intracellular membrane-bounded organelle	298	8346	490	17771	3.03E-10	6.20E-07
43227	membrane-bounded organelle	298	8353	490	17771	3.39E-10	6.20E-07
5739	mitochondrion	70	1273	490	17771	2.07E-08	2.52E-05
43229	intracellular organelle	315	9318	490	17771	5.06E-08	4.50E-05
43226	organelle	315	9332	490	17771	6.14E-08	4.50E-05
44424	intracellular part	355	10946	490	17771	2.00E-07	1.22E-04
34641	cellular nitrogen compound metabolic process	95	2078	490	17771	3.94E-07	2.07E-04
5634	nucleus	192	5184	490	17771	9.24E-07	3.85E-04
5622	intracellular	361	11300	490	17771	9.45E-07	3.85E-04
6807	nitrogen compound metabolic process	97	2196	490	17771	1.38E-06	5.05E-04
6139	nucleobase, nucleoside, nucleotide and nucleic acid metabolic process	80	1786	490	17771	8.48E-06	2.70E-03
33554	cellular response to stress	37	618	490	17771	8.83E-06	2.70E-03
5654	nucleoplasm	48	931	490	17771	2.29E-05	6.29E-03
90304	nucleic acid metabolic process	67	1460	490	17771	2.40E-05	6.29E-03
	Significant pathways enriched in 305 qualified transcripts down-regulated by G2						
5739	mitochondrion	59	1272	267	17786	3.59E-15	9.14E-12
5737	cytoplasm	157	7648	267	17786	1.23E-07	1.16E-04
44444	cytoplasmic part	117	5148	267	17786	1.37E-07	1.16E-04
44429	mitochondrial part	26	611	267	17786	1.87E-06	1.19E-03
46483	heterocycle metabolic process	17	337	267	17786	1.44E-05	7.04E-03
44281	small molecule metabolic process	41	1370	267	17786	1.66E-05	7.04E-03
	Top 10 significant pathways enriched in 304 qualified transcripts up-regulated by G2						
5634	nucleus	114	5185	223	17775	3.78E-12	9.31E-09
5488	binding	192	12356	223	17775	5.37E-09	6.61E-06

50789	regulation of biological process	122	6550	223	17775	3.66E-08	2.40E-05
5515	protein binding	142	8115	223	17775	3.90E-08	2.40E-05
50794	regulation of cellular process	117	6220	223	17775	5.71E-08	2.52E-05
3676	nucleic acid binding	74	3251	223	17775	6.15E-08	2.52E-05
44451	nucleoplasm part	25	585	223	17775	9.47E-08	3.33E-05
10468	regulation of gene expression	68	2926	223	17775	1.25E-07	3.60E-05
60255	regulation of macromolecule metabolic process	75	3375	223	17775	1.32E-07	3.60E-05
3677	DNA binding	58	2328	223	17775	1.49E-07	3.66E-05

Note: x, number of gene IDs identified in the designated pathway among input gene IDs; X, number of input gene IDs selected by BiNGO; n, number of known gene IDs in the designated pathway; N, number of background gene IDs selected from the GO pool by BiNGO. Replicated pathways in the subsequent pattern-based analyses are shown in red.

Supplemental Table 8. Pathways detected in pattern-based analysis ILLU using Cytoscape-based BiNGO for 1699 qualified genes

Pattern	Number of genes	GO-ID	Description	x	n	X	N	p-value	FDR p-value
1	71								
2	136								
3	67								
4	34								
5	158	5634	nucleus	74	5183	130	17783	3.30E-11	6.90E-08
		50794	regulation of cellular process	80	6221	130	17783	5.50E-10	5.76E-07
		50789	regulation of biological process	81	6551	130	17783	3.02E-09	1.35E-06
		31323	regulation of cellular metabolic process	57	3733	130	17783	3.54E-09	1.35E-06
		19219	regulation of nucleobase, nucleoside, nucleotide and nucleic acid metabolic process	50	3012	130	17783	3.67E-09	1.35E-06
		10468	regulation of gene expression	49	2925	130	17783	4.25E-09	1.35E-06
		51171	regulation of nitrogen compound metabolic process	50	3038	130	17783	4.94E-09	1.35E-06
		9889	regulation of biosynthetic process	50	3042	130	17783	5.17E-09	1.35E-06
		60255	regulation of macromolecule metabolic process	53	3374	130	17783	6.81E-09	1.55E-06
		10556	regulation of macromolecule biosynthetic process	48	2874	130	17783	7.42E-09	1.55E-06
6	393	5739	mitochondrion	87	1273	342	17780	2.80E-26	7.93E-23
		44444	cytoplasmic part	169	5147	342	17780	7.02E-16	9.92E-13
		44429	mitochondrial part	45	612	342	17780	9.48E-15	8.94E-12
		5737	cytoplasm	212	7644	342	17780	7.71E-13	5.45E-10
		43231	intracellular membrane-bounded organelle	222	8343	342	17780	1.05E-11	5.49E-09
		43227	membrane-bounded organelle	222	8350	342	17780	1.16E-11	5.49E-09
		44237	cellular metabolic process	147	4987	342	17780	1.72E-09	6.43E-07
		5740	mitochondrial envelope	30	437	342	17780	1.82E-09	6.43E-07
		43229	intracellular organelle	231	9318	342	17780	6.99E-09	2.05E-06
		44424	intracellular part	260	10947	342	17780	7.24E-09	2.05E-06
7	153								
8	96								

9	410	5634	nucleus	143	5181	317	17767	9.40E-10	2.19E-06
		44451	nucleoplasm part	34	585	317	17767	1.49E-09	2.19E-06
		5515	protein binding	195	8110	317	17767	7.50E-09	5.48E-06
		50794	regulation of cellular process	160	6212	317	17767	7.92E-09	5.48E-06
		50789	regulation of biological process	166	6542	317	17767	9.33E-09	5.48E-06
		90304	nucleic acid metabolic process	57	1460	317	17767	1.39E-08	6.79E-06
		44260	cellular macromolecule metabolic process	104	3507	317	17767	2.14E-08	8.96E-06
		60255	regulation of macromolecule metabolic process	100	3372	317	17767	4.66E-08	1.71E-05
		16604	nuclear body	17	191	317	17767	6.03E-08	1.97E-05
		19222	regulation of metabolic process	110	3914	317	17767	1.29E-07	3.40E-05
10	31								
11	54								
12	18								
13	71								
14	7								
5&9	564	5634	nucleus	215	5180	443	17761	2.83E-18	1.01E-14
		50794	regulation of cellular process	239	6210	443	17761	1.04E-16	1.85E-13
		50789	regulation of biological process	246	6540	443	17761	4.26E-16	5.08E-13
		60255	regulation of macromolecule metabolic process	152	3370	443	17761	7.76E-15	6.94E-12
		31323	regulation of cellular metabolic process	161	3729	443	17761	3.97E-14	2.84E-11
		19222	regulation of metabolic process	166	3912	443	17761	5.88E-14	3.51E-11
		5515	protein binding	279	8107	443	17761	8.57E-14	3.69E-11
		10468	regulation of gene expression	135	2922	443	17761	8.87E-14	3.69E-11
		65007	biological regulation	249	6927	443	17761	9.30E-14	3.69E-11
		44451	nucleoplasm part	48	585	443	17761	3.87E-13	1.39E-10
7&13	223	5739	mitochondrion	34	1272	191	17785	6.66E-07	1.34E-03
6,7 & 13	601	5739	mitochondrion	121	1273	533	17774	3.82E-31	1.33E-27
		44444	cytoplasmic part	248	5147	533	17774	2.30E-18	4.01E-15
		44429	mitochondrial part	62	612	533	17774	3.06E-17	3.55E-14
		43231	intracellular membrane-bounded organelle	340	8341	533	17774	1.44E-15	1.17E-12

		43227	membrane-bounded organelle	340	8348	533	17774	1.67E-15	1.17E-12
		5737	cytoplasm	318	7643	533	17774	3.17E-15	1.84E-12
		44237	cellular metabolic process	224	4986	533	17774	1.51E-12	7.54E-10
		43229	intracellular organelle	356	9316	533	17774	6.00E-12	2.62E-09
		43226	organelle	356	9330	533	17774	7.72E-12	2.93E-09
		44424	intracellular part	401	10944	533	17774	8.39E-12	2.93E-09

Note: x, number of gene IDs identified in the designated pathway among input gene IDs; X, number of input gene IDs selected by BiNGO; n, number of known gene IDs in the designated pathway; N, number of background gene IDs selected from the GO pool by BiNGO. FDR p value of 0.01 is defined as minimum significance for each listed pattern. For multiple significant pathways, only the top ten are included for each pattern.

Pathways significant in paired and pattern-based analyses are shown in red.

Supplemental Table 9. Pathways detected in pattern-based analysis AFFY using Cytoscape-based BiNGO for 3620 qualified genes

Pattern	Number of genes	GO-ID	Description	x	n	X	N	p-value	corr p-value
1	222	44085	cellular component biogenesis	24	1035	116	17786	4.47E-08	3.10E-05
		51276	chromosome organization	17	525	116	17786	5.20E-08	3.10E-05
		6334	nucleosome assembly	8	83	116	17786	6.73E-08	3.10E-05
		5634	nucleus	61	5185	116	17786	9.62E-08	3.10E-05
		31497	chromatin assembly	8	87	116	17786	9.76E-08	3.10E-05
		6333	chromatin assembly or disassembly	9	127	116	17786	1.45E-07	3.10E-05
		44428	nuclear part	31	1741	116	17786	1.47E-07	3.10E-05
		65004	protein-DNA complex assembly	8	92	116	17786	1.51E-07	3.10E-05
		34728	nucleosome organization	8	93	116	17786	1.65E-07	3.10E-05
		44260	cellular macromolecule metabolic process	47	3507	116	17786	2.00E-07	3.23E-05
2	1674	5739	mitochondrion	274	1272	1357	17736	9.68E-61	5.19E-57
		43231	intracellular membrane-bounded organelle	899	8330	1357	17736	3.57E-50	9.58E-47
		43227	membrane-bounded organelle	899	8337	1357	17736	5.61E-50	1.00E-46
		44424	intracellular part	1076	10922	1357	17736	5.39E-48	7.23E-45
		5622	intracellular	1091	11275	1357	17736	1.07E-44	1.15E-41
		8152	metabolic process	687	5931	1357	17736	3.45E-42	3.08E-39
		44237	cellular metabolic process	605	4971	1357	17736	4.81E-42	3.69E-39
		34641	cellular nitrogen compound metabolic process	329	2071	1357	17736	8.65E-42	5.80E-39
		44444	cytoplasmic part	613	5133	1357	17736	5.40E-40	3.22E-37
		6807	nitrogen compound metabolic process	337	2189	1357	17736	6.39E-40	3.43E-37
3	238	32502	developmental process	67	3234	185	17780	4.15E-09	1.11E-05
		7275	multicellular organismal development	62	2971	185	17780	1.65E-08	2.20E-05
		48856	anatomical structure development	56	2656	185	17780	7.96E-08	5.94E-05
		35295	tube development	16	297	185	17780	8.98E-08	5.94E-05

		9653	anatomical structure morphogenesis	34	1218	185	17780	1.11E-07	5.94E-05
		48731	system development	50	2422	185	17780	9.86E-07	4.39E-04
		50794	regulation of cellular process	96	6219	185	17780	1.59E-06	6.07E-04
		1657	ureteric bud development	7	60	185	17780	2.86E-06	9.54E-04
		50789	regulation of biological process	98	6549	185	17780	5.08E-06	1.51E-03
		65007	biological regulation	102	6938	185	17780	5.99E-06	1.60E-03
4	1206	5634	nucleus	543	5167	1020	17727	6.00E-62	3.06E-58
		10468	regulation of gene expression	364	2920	1020	17727	1.49E-53	3.79E-50
		60255	regulation of macromolecule metabolic process	398	3369	1020	17727	2.30E-53	3.92E-50
		50794	regulation of cellular process	588	6202	1020	17727	2.68E-52	3.41E-49
		10556	regulation of macromolecule biosynthetic process	357	2868	1020	17727	3.95E-52	4.03E-49
		19222	regulation of metabolic process	433	3910	1020	17727	3.22E-51	2.73E-48
		31323	regulation of cellular metabolic process	419	3727	1020	17727	7.38E-51	5.37E-48
		50789	regulation of biological process	603	6532	1020	17727	4.82E-50	3.07E-47
		9889	regulation of biosynthetic process	365	3035	1020	17727	9.04E-50	5.12E-47
		31326	regulation of cellular biosynthetic process	362	3012	1020	17727	3.41E-49	1.74E-46
5	63								
6	68								
7	21								
8	88	31323	regulation of cellular metabolic process	35	3734	69	17784	4.33E-08	5.66E-05
		19222	regulation of metabolic process	35	3917	69	17784	1.52E-07	6.70E-05
		5634	nucleus	41	5181	69	17784	1.54E-07	6.70E-05
		10468	regulation of gene expression	29	2927	69	17784	4.26E-07	1.19E-04
		45449	regulation of transcription	27	2621	69	17784	6.15E-07	1.19E-04

		80090	regulation of primary metabolic process	32	3553	69	17784	6.69E-07	1.19E-04
		60255	regulation of macromolecule metabolic process	31	3376	69	17784	7.39E-07	1.19E-04
		19219	regulation of nucleobase, nucleoside, nucleotide and	29	3013	69	17784	7.94E-07	1.19E-04
		6357	regulation of transcription from RNA polymerase II	14	747	69	17784	8.51E-07	1.19E-04
		51171	regulation of nitrogen compound metabolic process	29	3039	69	17784	9.54E-07	1.19E-04
9	7								
10	33								
1&2	1911	5739	mitochondrion	288	1272	1468	17733	3.07E-61	1.70E-57
		43231	intracellular membrane-bounded organelle	976	8330	1468	17733	9.56E-56	2.65E-52
		43227	membrane-bounded organelle	976	8337	1468	17733	1.57E-55	2.90E-52
		44424	intracellular part	1164	10921	1468	17733	4.77E-52	6.61E-49
		5622	intracellular	1180	11274	1468	17733	2.29E-48	2.54E-45
		8152	metabolic process	750	5929	1468	17733	3.45E-48	3.19E-45
		44237	cellular metabolic process	661	4970	1468	17733	5.82E-48	4.61E-45
		34641	cellular nitrogen compound metabolic process	360	2070	1468	17733	2.90E-47	2.01E-44
		6807	nitrogen compound metabolic process	369	2188	1468	17733	2.69E-45	1.65E-42
		43229	intracellular organelle	1020	9303	1468	17733	1.15E-43	6.35E-41
3&4	1665	50794	regulation of cellular process	728	6201	1346	17713	2.90E-50	1.69E-46
		5634	nucleus	640	5167	1346	17713	8.47E-50	2.47E-46
		50789	regulation of biological process	750	6530	1346	17713	1.55E-48	3.01E-45
		10468	regulation of gene expression	426	2920	1346	17713	7.90E-47	1.15E-43
		31323	regulation of cellular metabolic process	503	3726	1346	17713	9.94E-47	1.16E-43
		60255	regulation of macromolecule metabolic process	468	3369	1346	17713	3.37E-46	3.28E-43
		19222	regulation of metabolic process	518	3909	1346	17713	5.52E-46	4.61E-43
		10556	regulation of macromolecule biosynthetic process	418	2868	1346	17713	1.18E-45	8.61E-43

		9889	regulation of biosynthetic process	432	3035	1346	17713	1.10E-44	7.11E-42
		31326	regulation of cellular biosynthetic process	429	3012	1346	17713	2.20E-44	1.28E-41

Note: x, number of gene IDs identified in the designated pathway among input gene IDs; X, number of input gene IDs selected by BiNGO; n, number of known gene IDs in the designated pathway; N, number of background gene IDs selected from the GO pool by BiNGO. FDR p value of 0.01 is defined as minimum significance for each listed pattern. For multiple significant pathways, only the top ten are included for each pattern.

Pathways significant in paired and pattern-based analyses are shown in red.

Supplemental Table 10. Top pathways detected in pattern-based analysis AFFY using IPA

Pattern	Top Canonical pathways	FDR p-value	Target molecules in dataset
1&2	tRNA Charging	8.66E-23	CARS,GARS,DARS2,NARS2,FARSB,NARS,LARS,TARS2,FARS2,KARS,DARS,EARS2,VARS,SARS,SARS2,IARS,IARS2,RARS2,CARS2,MARS,FARSA,EPRS,WARS,RARS,YARS,AARS2,AARS
	Mitochondrial Dysfunction	2.49E-08	SDHB,ATP5H,NDUFA9,PSENEN,NDUFA7,COX6A1,COX8A,NDUFB5,ACO2,DHODH,NDUFB10,NDUFS1,SOD2,PARK7,ATPAF1,NDUFS2,CASP8,ATP5F1,NDUFAF1,UCP2,ATP5O,NDUFV3,SDHC,VDAC3,ATP5C1,COX11,NDUFV2,TXN2,UQCR10,CYC1,CAT,NDUFA12,CYB5A,COX15
	Valine Degradation I	7.04E-08	BCAT1,ECHS1,BCAT2,HIBADH,DLD,DBT,ACADSB,EHHADH,ALDH6A1,BCKDHB
	Isoleucine Degradation I	1.15E-06	BCAT1,ACAT2,ECHS1,BCAT2,DLD,ACAT1,ACADSB,EHHADH
	Oxidative Phosphorylation	1.50E-06	SDHB,ATP5H,NDUFA9,NDUFA7,COX6A1,ATP5O,NDUFV3,NDUFB5,COX8A,SDHC,NDUFB10,ATP5C1,NDUFS1,COX11,NDUFV2,UQCR10,CYC1,ATPAF1,NDUFA12,NDUFS2,CYB5A,ATP5F1,COX15
3 & 4	Molecular Mechanisms of Cancer	2.38E-11	RAF1,AXIN1,PIK3R1,SMAD3,TAB2,GSK3A,CCND1,RHOB,GNA13,NFKBIB,HIPK2,BIRC3,CDC25A,E2F4,CASP3,CREBBP,GNAZ,TCF3,RASGRF2,ADCY9,DAXX,CBL,GAB1,RND3,MAP2K3,NOTCH1,RAP1B,PIK3CA,BMP2,LRP6,GNA11,BMPR2,E2F3,NFKB1,BCL2,EP300,BRAF,JUN,NFKBIA,TGFB2,SMAD4,RHOF,MAP2K1,ITGB1,ARHGEF12,GNAQ,SMAD7,ADCY6,SIN3A,FZD8,FOS,PAK2,CDKN1A,RBPJ,BCL2L11,FZD7
	TGF-β Signaling	5.30E-10	RAF1,BMP2,SMAD3,CREBBP,SKI,SMAD7,BMPR2,ACVR2B,HOXC9,INHBB,EP300,SMURF1,BCL2,FOS,JUN,PIAS4,RNF111,TGFB2,SMAD4,SMURF2,MAP2K3,TFE3,MAP2K1
	ERK5 Signaling	1.48E-09	IL6ST,RPS6KB1,YWHAH,SGK1,CREBBP,GNAQ,MEF2A,EP300,FOS,GAB1,MEF2D,FOXO3,FOSL1,RPS6KA1,GNA13,WNK1,MAP3K3,ELK4,MAP3K2
	Glucocorticoid Receptor Signaling	2.76E-09	PBRM1,RAF1,PIK3CA,ARID1A,YWHAH,HSPA14,SGK1,NFATC3,SMAD3,PIK3R1,ARID2,NFKB1,EP300,BCL2,NFKBIA,NFAT5,JUN,CCL2,BAG1,PPP3R1,FOXO3,TGFB2,PRKAA2,SMAD4,TAF3,NFKBIB,MAP2K1,CXCL8,CREBBP,MAP3K1,HSPA2,NCOA3,HSPA8,TAF4B,FOS,POU2F1,TAF5,DUSP1,CDKN1A,FKBP4,NCOA1,SMARCC1,PHF10
	PTEN Signaling	2.92E-09	FOXO4,RAF1,PIK3CA,YWHAH,PIK3R1,TGFBR3,BMPR2,PDPK1,GSK3A,NFKB1,CCND1,BCL2,FOXO3,IGF1R,MAP2K1,ITGB1,RPS6KB1,CASP3,FGFR1,FOXG1,CNKSR3,CSNK2A2,CBL,CDKN1A,INSR,BCL2L11

Pathways significant in paired and pattern-based analyses are shown in red.

Supplemental Table 11. Most differentially expressed transcripts in primary tubular cells with two *APOL1* risk variants vs. homozygous G0

Gene Symbol	Description	Gene Fold Change	p-value
SEMA3A	sema domain, immunoglobulin domain (Ig), short basic domain, secreted, (semaphorin) 3A	-2.45	0.001082
PREX2	phosphatidylinositol-3,4,5-trisphosphate-dependent Rac exchange factor 2	-2.15	0.001715
NAPRT/NAPRT1	nicotinate phosphoribosyltransferase; nicotinate phosphoribosyltransferase domain containing 1	-1.96	0.002019
PIK3AP1	phosphoinositide-3-kinase adaptor protein 1	-1.9	0.004585
RAB19	RAB19, member RAS oncogene family	-1.89	0.000689
ATP5J	ATP synthase, H+ transporting, mitochondrial Fo complex, subunit F6; ATP synthase, H+ transporting, mitochondrial F0 complex, subunit F6	-1.88	0.000917
TRIM55	tripartite motif containing 55; tripartite motif-containing 55	-1.81	0.002754
FLOT1	flotillin 1	-1.74	0.000397
SEC14L1 SCARNA16 SNHG20 MIR6516 LINC00338	SEC14-like 1 (S. cerevisiae); small Cajal body-specific RNA 16; small nucleolar RNA host gene 20 (non-protein coding); microRNA 6516; long intergenic non-protein coding RNA 338	-1.71	0.000408
LOC100133331 LINC01001 LOC101929819 LOC388572 RP11-206L10.3	uncharacterized LOC100133331; long intergenic non-protein coding RNA 1001; putative uncharacterized protein encoded by LINC00174-like; uncharacterized LOC388572; novel transcript	-1.71	0.001442
HLA-H HLA-A	major histocompatibility complex, class I, H (pseudogene); major histocompatibility complex, class I, A	-1.68	0.002199
SLC44A4	solute carrier family 44, member 4	-1.67	0.001366
HLA-DQB1 XXbac-BPG254F23.6	major histocompatibility complex, class II, DQ beta 1; putative novel transcript	-1.62	0.001076
VARS	valyl-tRNA synthetase	-1.56	0.001477
BCAR3	breast cancer anti-estrogen resistance 3	-1.52	0.001427
UBALD2	UBA-like domain containing 2	-1.51	0.004272
HM13 MCTS2P	histocompatibility (minor) 13; malignant T cell amplified sequence 2, pseudogene	-1.5	0.004255
DNM1	dynamin 1	1.5	0.002191
ABHD13	abhydrolase domain containing 13	1.52	0.000011
ACN9	ACN9 homolog (S. cerevisiae)	1.55	0.00175
BPNT1	3(2), 5-bisphosphate nucleotidase 1; 3'(2'), 5'-bisphosphate nucleotidase 1	1.55	0.003687

PARK7	parkinson protein 7; Parkinson disease (autosomal recessive, early onset) 7	1.56	0.003173
MEST	mesoderm specific transcript; mesoderm specific transcript homolog (mouse)	1.57	0.003132
TMEM45A	transmembrane protein 45A	1.64	0.000339
RP13-131K19.1	novel transcript	1.64	0.002966
MIR202 MIR202HG	microRNA 202; MIR202 host gene (non-protein coding)	1.68	0.000036
ZEB2	zinc finger E-box binding homeobox 2; ZEB2 antisense RNA 1	1.69	0.00312
CNN2	calponin 2	1.71	0.000316
WRB	tryptophan rich basic protein	1.72	0.00135
CHIC1	cysteine-rich hydrophobic domain 1	1.76	0.001953
MEIS2	Meis homeobox 2	1.78	0.000329
FPGT-TNNI3K	FPGT-TNNI3K readthrough; fucose-1-phosphate guanylyltransferase; TNNI3 interacting kinase	1.79	0.004731
ZNF253	zinc finger protein 253	1.9	0.003295
TIMM13	translocase of inner mitochondrial membrane 13 homolog (yeast)	2.03	0.000023
SLC2A9	solute carrier family 2 (facilitated glucose transporter), member 9	2.06	0.001265
FILIP1L	filamin A interacting protein 1-like	2.24	0.001918
SLIT3	slit homolog 3 (Drosophila)	2.3	0.002095
LOC101927630 AC017060.1	uncharacterized LOC101927630; novel transcript	2.32	0.002769
CTSC	cathepsin C	2.35	0.004052
PDE1A	phosphodiesterase 1A, calmodulin-dependent	2.51	0.000152
OR2A9P OR2A20P OR2A1-AS1 LOC101928605 RP4-798C17.6	olfactory receptor, family 2, subfamily A, member 9 pseudogene; olfactory receptor, family 2, subfamily A, member 20 pseudogene; OR2A1 antisense RNA 1; uncharacterized LOC101928605; novel transcript, antisense to OR2A9P, OR2A1 and ARHGEF5	2.69	0.000363
FGB	fibrinogen beta chain	44.95	0.004883

Note: Significant threshold is set at absolute fold change greater than 1.5 and p value less than 0.005. Gene IDs shown in red are replicated transcripts identified in HEK293 Tet-on cell pattern analysis. NAPRT/NAPRT1 falls into pattern 7 and ZEB2 into pattern 9 in Supplemental Table 8.

Supplemental Table 12. Primary antibodies used in immunoblot and immunofluorescence

Antibody	Vendor	Catalog #	Host species	Dilution
Immunoblot				
APOL1	Lampire	Custom designed ref Weckerle et al., JLR	rabbit	1:1,000
COXIV	Cell Signaling	4850	rabbit	1:1,000
Porin/VDAC1	Abcam	ab14734	mouse	1:1,000
β-actin	Sigma	A5441	mouse	1:10,000
Immunofluorescence				
APOL1	Epitomics	3245-1	rabbit	1:1,000
ATP5A1	Invitrogen	439800	mouse	1:1,000